ULTIMATE LIMIT STATE ANALYSIS AND DESIGN OF PLATED STRUCTURES

SECOND EDITION

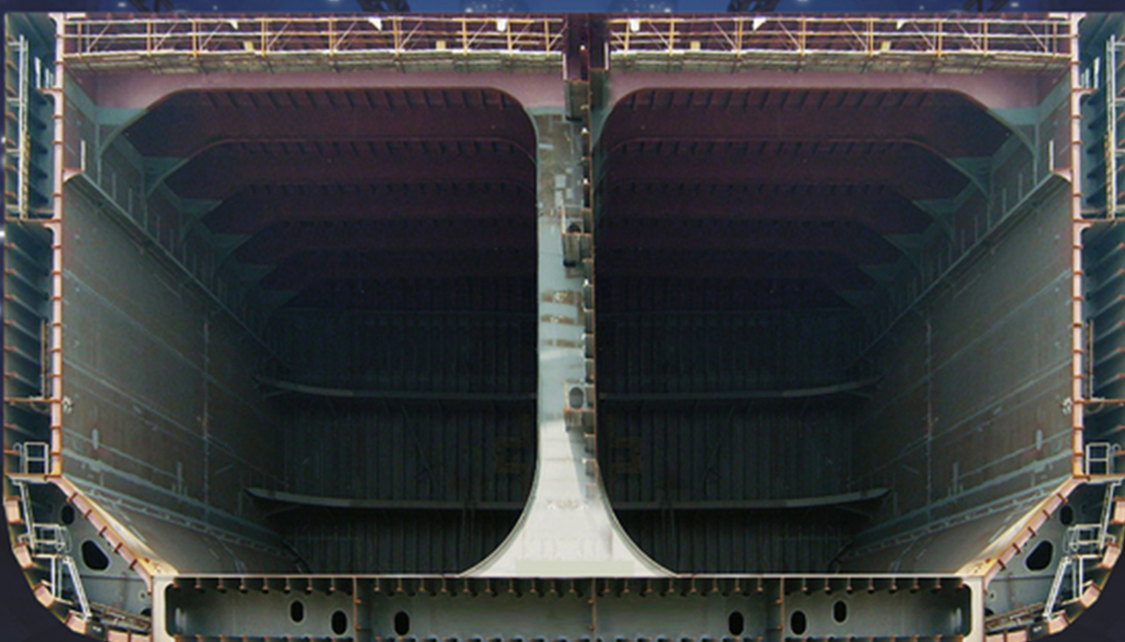

JEOM KEE PAIK

WILEY

Ultimate Limit State Analysis and Design of Plated Structures

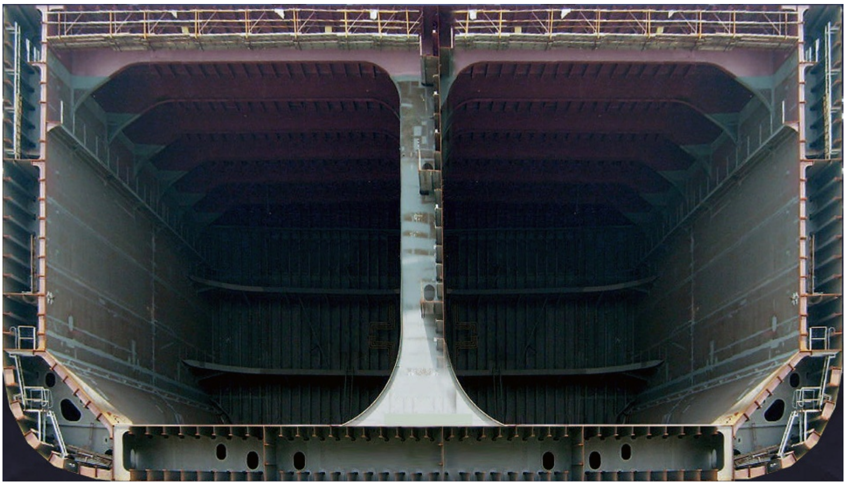

Ultimate Limit State Analysis and Design of Plated Structures

Second Edition

Jeom Kee Paik

Department of Naval Architecture and Ocean Engineering at Pusan National University, Korea
Department of Mechanical Engineering at University College London, UK

WILEY

This edition first published 2018

Edition History
Ultimate Limit State Design of Steel-Plated Structures, Edition One. January 2003. ISBN: 978-0-471-48632-9. Jeom Kee Paik, Anil Kumar Thayamballi.

Registered Offices
John Wiley & Sons, Inc., 111 River Street, Hoboken, NJ 07030, USA
John Wiley & Sons Ltd, The Atrium, Southern Gate, Chichester, West Sussex, PO19 8SQ, UK

Editorial Office
The Atrium, Southern Gate, Chichester, West Sussex, PO19 8SQ, UK

For details of our global editorial offices, customer services, and more information about Wiley products visit us at www.wiley.com.

Wiley also publishes its books in a variety of electronic formats and by print-on-demand. Some content that appears in standard print versions of this book may not be available in other formats.

Library of Congress Cataloging-in-Publication Data

Names: Paik, Jeom Kee, author.
Title: Ultimate limit state analysis and design of plated structures / Jeom Kee Paik.
Description: 2nd edition. | Hoboken, NJ : John Wiley & Sons, 2018. | Includes index. |
Identifiers: LCCN 2017046042 (print) | LCCN 2017056354 (ebook) | ISBN 9781119367765 (pdf) | ISBN 9781119367789 (epub) | ISBN 9781119367796 (cloth)
Subjects: LCSH: Building, Iron and steel. | Plates, Iron and steel.
Classification: LCC TA684 (ebook) | LCC TA684 .P24 2018 (print) | DDC 624.1/821–dc23
LC record available at https://lccn.loc.gov/2017046042

Cover design: Wiley
Cover image: (Background) © fredmantel/Gettyimages; (Inset image) Courtesy of Jeom Kee Paik

Set in 10/12pt Warnock by SPi Global, Pondicherry, India

10 9 8 7 6 5 4 3 2 1

Contents

Preface

Plated structures are important in a variety of marine- and land-based applications, including ships, offshore platforms, box girder bridges, power/chemical plants, and box girder cranes. The basic strength members in plated structures include support members (such as stiffeners and plate girders), plates, stiffened panels, grillages, box columns, and box girders. During their lifetimes, the structures constructed with these members are subjected to various types of actions and action effects that are usually normal but sometimes extreme or even accidental.

In the past, criteria and procedures for designing plated structures were primarily based on allowable working stresses and simplified buckling checks for structural components. However, it is now well recognized that the limit state approach is a better basis for design because it is difficult to determine the real safety margin of any structure using linear elastic methods alone. It also readily follows that it is of crucial importance to determine the true limit state if one is to obtain consistent measures of safety that can then form a fairer basis for comparison of structures of different sizes, types, and characteristics. An ability to better assess the true margin of safety would also inevitably lead to improvements in related regulations and design requirements.

Today, the preliminary design of ships including naval and merchant vessels, offshore structures such as ship-shaped offshore installations, mobile offshore drilling units, fixed-type offshore platforms and tension leg platforms, and land-based structures such as bridges and box girder cranes tends to be based on limit state considerations, including the ultimate limit state.

To obtain a safe and economic structure, the limit state-based capacity and structural behavior under known loads must be assessed accurately. The structural designer can perform such a relatively refined structural safety assessment even at the preliminary design stage if simple expressions are available for accurate prediction of the limit state behavior. A designer may even desire to do this for not only the intact structure but also structures with premised damage to assess their damage tolerance and survivability.

Although most structural engineers in the industry are very skilled and well experienced in the practical structural design aspects based on the traditional criteria, they may need a better background in the concept of limit state design and related engineering tools and data. Hence, there is a need for a relevant engineering book on the subject that provides an exposition of basic knowledge and concepts. Many structural specialists in research institutes continue to develop more advanced methods for the limit state design of plated structures, but they sometimes lack the useful engineering data to validate them. Students in universities want to learn more about the fundamentals and practical procedures regarding the limit state analysis and design and thus need a book that provides useful insights into the related disciplines.

This book reviews and describes both the fundamentals and practical procedures for the ultimate limit state analysis and design of ductile steel-plated and aluminum-plated structures. Structural fracture mechanics and structural impact mechanics are also described. This book is an extensive update of my previous book *Ultimate Limit State Design of Steel-Plated Structures* (with Dr. A.K. Thayamballi), published in 2003. In contrast to the previous book, this update covers both steel- and aluminum-plated structures together with the latest advances and many newly added materials not included in the 2003 version. The book is basically designed as a textbook. The derivation of the basic mathematical expressions is presented together with a thorough discussion of the assumptions and the validity of the underlying expressions and solution methods.

I believe that the reader should be able to obtain insight into a wider spectrum of ultimate limit state analysis and design considerations in both an academic and a practical sense. In part, this book is an easily accessible analysis and design toolbox that facilitates learning by applying the concepts of the ultimate limit state for practice.

This book is primarily based on my own insights and developments obtained from more than 35 years of professional experience, as well as information and findings provided by numerous other researchers and limit state design practitioners. Wherever possible, I have tried my best to acknowledge the invaluable efforts of other investigators and practitioners, and, if I have failed anywhere in this regard, I did so inadvertently.

I gratefully acknowledge all those individuals who helped make this book possible. Most of all, Dr. A.K. Thayamballi, who was the coauthor of the previous book, provided valuable and comprehensive comments to improve this book. Finally, I take this opportunity to thank my wife Yun Hee Kim, my son Myung Hook Paik and my daughter Yun Jung Paik for their unfailing patience and support while this book was being written.

October 2017

Prof. Jeom Kee Paik, Dr. Eng., CEng, DHC (ULieg), FRINA, LFSNAME
Pusan National University
and University College London

About the Author

Dr. Jeom Kee Paik is a professor and faculty member of both the Department of Naval Architecture and Ocean Engineering of Pusan National University (PNU) in Korea and the Department of Mechanical Engineering of University College London in the United Kingdom. He is an honorary professor both at University of Strathclyde in the United Kingdom and at Southern University of Science and Technology in China. He was a visiting professor at Technical University of Denmark, Virginia Polytechnic Institute and State University, USA, and University of Newcastle, Australia.

Prof. Paik founded two key institutions: the Korea Ship and Offshore Research Institute (KOSORI) (http://www.kosori.org) at PNU, which has been a Lloyd's Register Foundation Research Centre of Excellence (ICASS, International Centre for Advanced Safety Studies, http://www.icass.kr) since 2008, and the Forum for Safety of Fire and Explosion (http://www.safeforum.co.kr) under the Ministry of Interior and Safety of Korea. He also serves as president and chairman, respectively. He is founder and editor-in-chief of *Ships and Offshore Structures* (http://saos.edmgr.com), which is a peer-reviewed international journal published by Taylor & Francis, UK. He is cofounder and cochairman of the International Conference on Ships and Offshore Structures (http://www.iscos.info), which is an annual event associated with the *Ships and Offshore Structures* journal.

Prof. Paik received Bachelor of Engineering degree from Pusan National University, Korea and Master of Engineering and Doctor of Engineering degrees from Osaka University, Japan. Prof. Paik is a life fellow, fellows committee member, Marine Technology board member, and vice president of the US Society of Naval Architects and Marine Engineers (SNAME), and a fellow, council member, publications committee member, and Korean branch chairman of the UK Royal Institution of Naval Architects (RINA).

Prof. Paik's research interests include nonlinear structural mechanics, analysis, and design; advanced safety studies; limit state-based design; structural reliability; risk assessment and management; health condition assessment and management; fires, explosions, collisions, grounding, dropped objects, and impact engineering; corrosion assessment and management; structural longevity; inspection and maintenance; and decommissioning.

Prof. Paik has authored or coauthored more than 500 technical papers including over 270 peer-reviewed journal articles. He is the coauthor or coeditor of four books: *Ultimate Limit State Design of Steel-Plated Structures* (with A.K. Thayamballi), John Wiley & Sons, 2003; *Ship-Shaped Offshore Installations: Design, Building, and Operation* (with A.K. Thayamballi), Cambridge University Press, 2007; *Condition Assessment of Aged Structures* (with R.E. Melchers), CRC Press, 2009; and *Ship Structural Analysis and Design* (with O.F. Hughes), SNAME, 2013. He also obtained numerous patents based on his research studies over a wide range of topics in naval architecture and ocean engineering.

Among other recognitions, Prof. Paik received both the William Froude Medal of the RINA (2015) and the David W. Taylor Medal of the SNAME (2013), the two most prestigious medals in the global maritime community in recognition for his contributions to naval architecture and ocean engineering. He was conferred the Doctor Honoris Causa (Honorary Doctorate) by the University of Liege in Belgium (2012) in recognition for his contributions to international science, engineering, and technology. Prof. Paik was awarded the Republic of Korea Order of Science and Technology Merit (2014). He has received numerous (13) best paper awards and engineering prizes from the SNAME, the RINA, the UK Institution of Mechanical Engineers, the American Society of Mechanical Engineers, and the Society of Naval Architects of Korea. He was also awarded the Kyung-Ahm Prize (2013) from the Kyung-Ahm Education and Culture Foundation. As a very special honor for a living figure, the RINA created a prize named in honor of Prof. Paik, the *Jeom Kee Paik Prize*, which has been awarded each year since 2015 for the best paper on structures published by a researcher under 30 years of age; the prize is the first of its kind named for a non-Briton in the RINA's 156-year history.

Prof. Paik has served in numerous international engineering societies in various capacities. He served as editor-in-chief of UNESCO's Encyclopedia of Life Support System with EOLSS 6.177 Ships and Offshore Structures in 2006–2011. He served as chairman of the Korean Shipbuilding Advisory Committee of Registro Italiano Navale (Italian Classification Society) in 2013–2014 and the numerous technical committees of the International Ship and Offshore Structures Congress (ISSC) associated with Ship Collisions and Grounding (2000–2003), Condition Assessment of Aged Ships (2003–2006), and Ultimate Strength (2006–2012). He has presided numerous international conferences, including the International Conference on Thin-Walled Structures (ICTWS 2014, Busan, Korea) and the International Conference on Ocean, Offshore, and Arctic Engineering (OMAE 2016, Busan, Korea), and has cochaired the International Conferences on Ships and Offshore Structures. He will chair the upcoming International Symposium on Plasticity and Impact Mechanics (IMPLAST 2019, Busan, Korea). Currently, Prof. Paik heads the Korean Technical Committee of ClassNK (Japanese Classification Society), is a member of the Academic Advisory Council of Universiti Teknologi PETRONAS in Malaysia and of the ISSC Standing Committee, and is an editorial board member for more than 20 international journals.

How to Use This Book

Written to develop a textbook and handy source for the principles behind the ultimate limit state analysis and design of steel- and aluminum-plated structures, this book is designed to be well suited for university students approaching the related technologies. In terms of the more advanced and sophisticated analysis and design methodologies presented, this book should also meet the needs of structural analysts, designers, or researchers involved in the field of naval architecture and offshore, civil, architectural, aerospace, and mechanical engineering.

Hence, apart from its value as a ready reference and an aid to continuing education for established practitioners, this book can be used as a textbook for teaching courses on ultimate limit state analysis and design of plated structures at the university level, as it covers a wide enough range of topics that may be considered for more than one semester course.

A teaching course of 45 h for undergraduate students in structural mechanics or thin-walled structures may cover Chapter 1, "Principles of Limit State Design"; Chapter 2, "Buckling and Ultimate Strength of Plate–Stiffener Combinations: Beams, Columns, and Beam–Columns"; Chapter 3, "Elastic and Inelastic Buckling Strength of Plates Under Complex Circumstances"; Chapter 5, "Elastic and Inelastic Buckling Strength of Stiffened Panels and Grillages"; Chapter 7, "Buckling and Ultimate Strength of Plate Assemblies: Corrugated Panels, Plate Girders, Box Columns, and Box Girders"; and Chapter 8, "Ultimate Strength of Ship Hull Structures."

For postgraduate students who pass the teaching course for the undergraduate students noted previously, a more advanced course of 45 h may cover Chapter 1, "Principles of Limit State Design" (repeated); Chapter 2, "Buckling and Ultimate Strength of Plate–Stiffener Combinations: Beams, Columns, and Beam–Columns" (repeated); Chapter 4, "Large Deflection and Ultimate Strength Behavior of Plates"; and Chapter 6, "Large Deflection and Ultimate Strength Behavior of Stiffened Panels and Grillages."

In teaching courses, lecturers are advised to guide students to practice the derivations of important formulations described in each chapter together with practical problems for analysis and design of steel- and aluminum-plated structures. Students may submit homework reports to the lecturers, an exercise that would be helpful for students to better understand the fundamentals and practical applications.

Chapter 9, "Structural Fracture Mechanics," and Chapter 10, "Structural Impact Mechanics," should also be useful in association with fatigue limit state design and accidental limit state design, respectively. These two chapters are supplementary for the ultimate limit state analysis and design, as they describe the fundamentals and practices of fatigue and accidental limit states. Chapter 11, “The Incremental Galerkin Method”; Chapter 12, “The Nonlinear Finite Element Method”; and Chapter 13, “The Intelligent Supersize Finite Element Method,” should be useful for postgraduate students, researchers, and practicing engineers given their more refined and sophisticated analyses of the ultimate strength behavior of plated structures.

The author has attempted to fulfill these many lofty aims in developing this book. He sincerely hopes his efforts prove successful, however modestly.

1

Principles of Limit State Design

1.1 Structural Design Philosophies

While in service, structures are likely to be subjected to various types of loads (or actions) and load effects (or action effects) due to operational and environmental conditions that are usually normal but are sometimes extreme or even accidental. The mission of the structural designer is to design a structure that can withstand the operational and environmental requirements designated throughout its expected lifetime.

The load effects or maximum load-carrying capacities or limit states of a structure are affected by a variety of factors that essentially involve a great deal of uncertainty, which include the following:

- Geometric factors associated with structural characteristics, buckling, large deformation, crushing, or folding
- Material factors associated with chemical composition, mechanical properties, yielding or plasticity, or fracture
- Fabrication related initial imperfections, such as initial distortion, welding induced residual stress, or softening
- Temperature factors, such as low temperatures associated with operation in cold waters or low-temperature cargo and high temperatures due to fire and explosions
- Dynamic or impact factors (e.g., strain rate sensitivity or inertia effect) associated with freak waves and impact pressure actions that arise from sloshing, slamming, or green water; overpressure actions that arise from explosion; and impact from collisions, grounding, or dropped objects
- Age related degradation factors, such as corrosion or fatigue cracking
- Accident induced damage factors, such as local denting, collision damage, grounding damage, fire damage, or explosion damage
- Human factors related to unusual operations (e.g., ship's operational speed compared with maximum permitted speed or acceleration, ship's heading, or loading or unloading conditions)

Uncertainties can comprise two groups: inherent uncertainties and modeling uncertainties. Inherent uncertainties are caused by natural variabilities in environmental actions and material properties, and modeling uncertainties arise from inaccuracy in engineering modeling associated with the evaluation and control of loads, load effects

Ultimate Limit State Analysis and Design of Plated Structures, Second Edition. Jeom Kee Paik.

(e.g., stress, deformation), load-carrying capacities, or limit states and from variations in building and operational procedures. In design, a structure is thus required to have an adequate margin of safety against service requirements because of such inherent and modeling uncertainties.

A "demand" is analogous to load, and a "capacity" is analogous to the strength necessary to resist that load, both measured consistently (e.g., as stress, deformation, resistive or applied load or moment, or energy either lost or absorbed). In this regard, a performance function G of a structure can be given as follows:

$$G = C_d - D_d \tag{1.1a}$$

where C_d represents the "design" capacity and D_d represents the "design" demand. The terminology "design" implies that both demand and capacity are determined by accounting for the inherent and modeling uncertainties.

Because both C_d and D_d in Equation (1.1a) are a function of the basic variables, $X = (x_1, x_2, \ldots, x_i, \ldots, x_n)$, the performance function G can be rewritten as follows:

$$G = G(X) = G(x_1, x_2, \ldots, x_i, \ldots, x_n) \tag{1.1b}$$

When $G(X) > 0$, the structure is in the desired state. When $G(X) \le 0$, the structure is in the undesired state. In industry practice, the performance function of a structure is sometimes defined in an opposite manner to Equation (1.1a) as follows:

$$G^* = D_d - C_d \tag{1.2}$$

where G^* is the performance function of a structure. In this case, the structure is in the desired state when $G^* < 0$, and it is in the undesired state when $G^* \ge 0$. Figure 1.1 illustrates the two performance functions associated with the desired and undesired states.

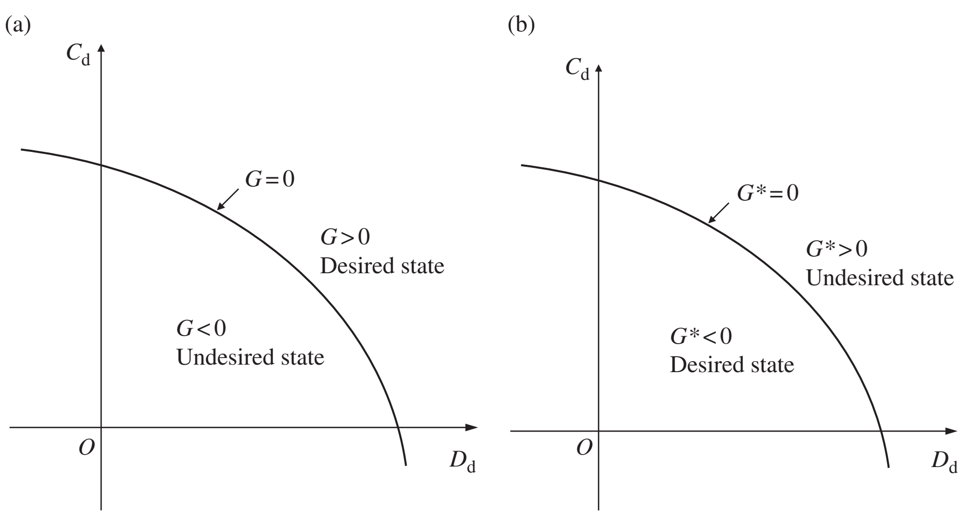

Figure 1.1 The performance functions associated with the desired and undesired states: (a) a performance function G, Equation (1.1a); (b) a performance function G^*, Equation (1.2).

1.1.1 Reliability-Based Design Format

The reliability-based design format usually involves the following tasks:

1) Definition of a target reliability
2) Identification of all unfavorable failure modes of the structure
3) Formulation of the limit state (performance) function for each failure mode identified in item (2)
4) Identification of the probabilistic characteristics (mean, variance, probability density distribution) of the random variables in the limit state function
5) Calculation of the reliability against the limit state with respect to each failure mode of the structure
6) Evaluation of the predicted reliability whether or not it is greater than the target reliability
7) Redesign of the structure otherwise
8) Evaluation of the reliability analysis results with respect to a parametric sensitivity consideration

Each of the basic variables in the reliability-based design format is dealt with in a probabilistic manner as a random parameter, where each random variable must be characterized by the corresponding probability density function that has a mean value and standard deviation. If the first-order approximation is adopted, the performance function $G(X)$ can be rewritten by the Taylor series expansion as follows:

$$G(X) \cong G(\mu_{x1}, \mu_{x2}, \ldots, \mu_{xi}, \ldots, \mu_{xn}) + \sum_{i=1}^{n} \left(\frac{\partial G}{\partial x_i} \right)_{\bar{x}} (x_i - \mu_{xi}) \tag{1.3}$$

where μ_{xi} is the mean value of the variable x_i, $\bar{x}$ is the mean value of the basic variables = $(\mu_{x1}, \mu_{x2}, \ldots, \mu_{xi}, \ldots, \mu_{xn})$, and $(\partial G/\partial x_i)_{\bar{x}}$ is the partial differentiation of $G(X)$ with respect to x_i at $x_i = \mu_{xi}$.

The mean value of the performance function $G(X)$ is then given by

$$\mu_G = G(\mu_{x1}, \mu_{x2}, \ldots, \mu_{xi}, \ldots, \mu_{xn}) \tag{1.4}$$

where μ_G represents the mean value of the performance function $G(X)$.

The standard deviation of the performance function $G(X)$ is calculated by

$$\sigma_G = \left[\sum_{i=1}^{n} \left(\frac{\partial G}{\partial x_i} \right)_{\bar{x}}^2 \sigma_{xi}^2 + 2 \sum_{i>j} \left(\frac{\partial G}{\partial x_i} \right)_{\bar{x}} \left(\frac{\partial G}{\partial x_j} \right)_{\bar{x}} \mathrm{covar}\left(x_i, x_j\right) \right]^{1/2} \tag{1.5a}$$

where σ_G is the standard deviation of $G(X)$, σ_{x_i} is the standard deviation of the variable x_i, $\mathrm{covar}\left(x_i, x_j\right) = E\left[(x_i - \mu_{xi}) \left(x_j - \mu_{xj} \right) \right]$ is the covariation of x_i and x_j, and $E[]$ is the mean value of [ ].

When the basic variables $X = (x_1, x_2, \ldots, x_i, \ldots, x_n)$ are independent of each other, $\mathrm{covar}(x_i, x_j) = 0$. In this case, Equation (1.5a) is simplified to

$$\sigma_G = \left[\sum_{i=1}^{n} \left(\frac{\partial G}{\partial x_i} \right)_{\bar{x}}^2 \sigma_{xi}^2 \right]^{1/2} \tag{1.5b}$$

If the so-called first-order second-moment method (Benjamin & Cornell 1970) is adopted, the reliability index for this case can be determined as follows:

$$\beta = \frac{\mu_G}{\sigma_G} \tag{1.6}$$

where β represents the reliability index.

For a simpler case with a performance function $G(X)$ of two parameters, for example, capacity C and demand D, that are considered to be statistically independent, the reliability index β can be calculated as follows:

$$\mu_G = \mu_C - \mu_D \tag{1.7a}$$

$$\sigma_G = \sqrt{(\sigma_C)^2 + (\sigma_D)^2} \tag{1.7b}$$

$$\beta = \frac{\mu_C - \mu_D}{\sqrt{(\sigma_C)^2 + (\sigma_D)^2}} = \frac{\mu_C/\mu_D - 1}{\sqrt{(\mu_C/\mu_D)^2(\eta_C)^2 + (\eta_D)^2}} \tag{1.7c}$$

where μ_C or μ_D are the mean values of C or D, σ_C or σ_D are the standard deviations of C or D, and η_C or η_D are the coefficients of variation (i.e., the standard deviation divided by the mean value) of C or D.

To achieve a successful design, the reliability index should be greater than a target reliability index:

$$\beta \geq \beta_T \tag{1.8}$$

where β_T is the target reliability.

The target reliability or the required level of structural reliability may vary from one industry to another depending on various factors such as the type of failure, the seriousness of its consequence, or public and media sensitivity. Appropriate values of target reliability are not readily available and are usually determined by surveys or by examinations of the statistics on failures although the fundamental difference between a risk assessment and a reliability analysis needs to be acknowledged when interpreting such results. The methods to select the target safeties and reliabilities may be categorized into the following three groups (Paik & Frieze 2001):

- "Guesstimation": A "reasonable" value as recommended by a regulatory body or professionals on the basis of successful prior experience. This method may be employed for the new types of structure for which statistical database on failures does not exist.
- Calibration of design rules: The level of reliability is estimated by calibrating a new design rule to an existing successful one. This method is normally used for the revisions of existing design rules.
- Economic value analysis: The target reliability is selected to minimize total expected costs during the service life of the structure.

For elaborate descriptions in reliability analysis, interested readers may refer to Benjamin and Cornell (1970), Nowak and Collins (2000), Melchers (1999a), and Modarres et al. (2016), among others.

1.1.2 Partial Safety Factor-Based Design Format

In the partial safety factor-based design format, the design capacity or demand is defined by considering the corresponding partial safety factors that are associated with the inherent and modeling uncertainties. A characteristic or nominal value of capacity C_k or demand D_k is determined as the mean value of the corresponding random variable. A design capacity C_d or demand D_d is, however, defined to suit a specified percentage of the area below the probability curve for the corresponding random variable. For instance, a design strength or capacity C_d can be defined for a lower bound or 95% exceedance value, whereas a design load or demand D_d can be defined for an upper bound or a 5% exceedance value, as shown in Figure 1.2. In this regard, the design capacity or demand is defined as follows:

$$C_d = \frac{C_k}{\gamma_C} \tag{1.9a}$$

$$D_d = \gamma_D D_k \tag{1.9b}$$

where C_k is the characteristic (or nominal) value of capacity or μ_C in Equation (1.7a), D_k is the characteristic (or nominal) value of demand or μ_D in Equation (1.7a), γ_C is the partial safety factor associated with capacity, and γ_D is the partial safety factor associated with demand. Because the partial safety factors must be greater than 1.0, it is obvious that the characteristic value of capacity C_k is reduced and the characteristic value of demand D_k is amplified to determine their design values, C_d or D_d.

The measure of structural adequacy η can be determined as follows:

$$\eta = \frac{C_d}{D_d} = \frac{1}{\gamma_C \gamma_D} \frac{C_k}{D_k} \tag{1.10}$$

To achieve a successful design, the measure of structural adequacy η must be greater than 1.0 by a sufficient margin as follows:

$$\eta = \frac{C_d}{D_d} = \frac{1}{\gamma_C \gamma_D} \frac{C_k}{D_k} > 1 \tag{1.11}$$

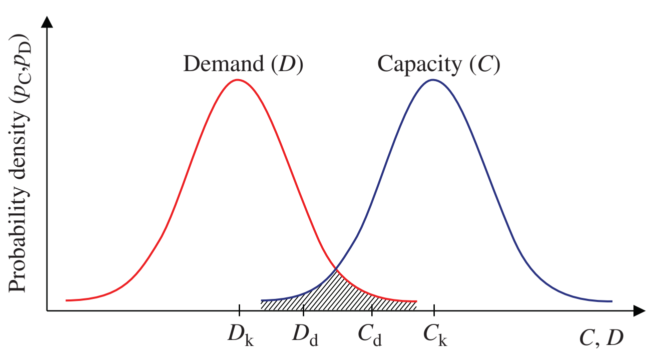

Figure 1.2 Probability density distributions of capacity and demand.

1.1.3 Failure Probability-Based Design Format

Whatever the level of uncertainty, every structure may have some probability of failure, which is the possibility of a load or demand exceeding its limit value or capacity. The probability of failure P_f for a particular type of failure in association with the performance function G, Equation (1.1), or G^*, Equation (1.2), is defined as follows:

$$\text{Probability of failure} \quad P_{\mathrm{f}} = \mathrm{prob}(G \le 0) = \mathrm{prob}(G^* \ge 0) = \mathrm{prob}(C_{\mathrm{d}} \le D_{\mathrm{d}}) \tag{1.12a}$$

The safety of a structure is the converse, which is the probability that it will not fail, namely,

$$\text{Safety} = \mathrm{prob}(G > 0) = \mathrm{prob}(G^* < 0) = \mathrm{prob}(C_{\mathrm{d}} > D_{\mathrm{d}}) = 1 - P_{\mathrm{f}} \tag{1.12b}$$

The probability of failure can generally be calculated as follows:

$$P_{\mathrm{f}} = \int_{G \le 0} p_x(X)dx = \int_{G^* \ge 0} p_x^*(X)dx \tag{1.13}$$

where $p_x(X)$ and $p_x^*(X)$ are the joint probability density functions of the random variables, $X = (x_1, x_2, \ldots, x_i, \ldots, x_n)$, associated with demand and capacity, and $G(X)$ or $G^*(X)$ is the limit state (performance) function defined such that negative or positive values imply failure, respectively.

Since $G(X)$ or $G^*(X)$ is usually a complicated nonlinear function, it is not straightforward to perform the direct integration of Equation (1.13) associated with the joint probability density function, $p_x(X)$ or $p_x^*(X)$. Therefore, Equation (1.13) is often solved with approximate procedures, where the limit state (performance) function $G(X)$ or $G^*(X)$ is approximated at the design point by either a tangent hyperplane or hyperparabola, which simplifies the mathematics related to the calculation of failure probability. The first type of approximation with the tangent hyperplane is called the first-order reliability method (FORM), and the second type with the hyperparabola is called the second-order reliability method (SORM). Such methods facilitate the rapid calculation of the probability of failure by widely available standard software packages. In addition to the individual probability distributions of the random variables involved, the correlation between the "A" and "B" parameters can also be readily accounted for in such calculations.

Considering the probability density distributions of capacity and demand, as illustrated in Figure 1.2, the probability of a particular type of failure can be calculated as follows:

$$P_{\mathrm{f}} = \int_0^{\infty} \left[\int_0^{y} p_{\mathrm{C}}(x)dx \right] p_{\mathrm{D}}(y)dy \tag{1.14}$$

where $p_{\mathrm{C}}(x)$ is the probability density function of capacity associated with a variable x and $p_{\mathrm{D}}(y)$ is the probability density function of demand associated with a variable y.

Although the mean value of capacity C_{k} is much greater than the mean value of demand D_{k}, there is still some possibility that the capacity is less than the demand. It is usually challenging to compute Equation (1.14), but it is interesting to note that the shaded area of the overlap in Figure 1.2 indicates an approximation of the probability of failure P_{f}. To achieve a successful design, the probability of failure should be minimized to a sufficiently low value.

1.1.4 Risk-Based Design Format

The risk-based design format usually involves the following five tasks: (i) hazard identification, (ii) risk calculation, (iii) establishment of a set of potential risk control options, (iv) cost–benefit analysis for the risk control options, and (v) decision making. In engineering community, risk is defined as a product of the frequency of the hazard and the level of consequence as follows:

$$R = F \times C \tag{1.15}$$

where R is the risk, F is the frequency of the hazard, and C is the level of consequence.

The frequency of the hazard represents the likelihood that the hazard will occur, and the level of consequence represents the impact or severity of consequence, indicating how bad the consequences would be if the hazard did occur in terms of casualties, property damage, and environmental pollution. The frequency of a hazard is usually measured by the number of occurrences per unit time (e.g., per year). The level of consequence is sometimes measured on a monetary basis (e.g., repair costs for accidental damage or insurance costs for pollution).

The characterization of the frequency and the consequences is required for risk assessment. Qualitative risk assessment techniques use simple methods that do not require numerical computations, but quantitative risk assessment requires more refined methods associated with numerical and experimental investigations. It is of course much more desirable to apply the quantitative risk assessment methods for more precise calculations of the risks in association with casualties, property damage, and environmental pollution.

According to Equation (1.15), it is obvious that one may need to reduce F or C or both to reduce risks. To achieve a successful design, fabrication, or operation, the risk should be minimized to an "as low as reasonably practicable (ALARP)" level. Undertaking activities to control risks is risk management, which involves risk control options. Cost–benefit analysis is undertaken to make a ranking between a set of potential risk control options, and a single or multiple options should be applied to best control the risks to meet the ALARP level. Risk assessment and management are recognized as the best tools for decision making in association with robust design, building, operation, or decommissioning of structures.

1.2 Allowable Stress Design Versus Limit State Design

Limit state design differs from the traditional allowable stress design. In the allowable stress design, the focus is on keeping the stresses from the design loads under a certain working stress level, which is usually based on successful similar experience. In industry practice, regulatory bodies or classification societies usually specify the value of the allowable stress as some fraction of the mechanical properties of materials (e.g., yield strength). The criterion of the allowable stress design is typically given by

$$\sigma < \sigma_{\mathrm{a}} \tag{1.16}$$

where σ is the working stress and σ_{a} is the allowable stress.

In contrast to the allowable stress design, the limit state design is based on explicit consideration of the various conditions under which the structure may cease to fulfill its intended function. For these conditions, the applicable capacity or strength is estimated and used during design as a limit for such behavior.

For this purpose, a structure's load-carrying capacity is normally evaluated with simplified design formulations or more refined computations such as nonlinear elastic–plastic large-deformation finite element analyses with appropriate modeling related to geometric or material properties, initial imperfections, boundary conditions, load application, and finite element mesh sizes, as appropriate.

During the past several decades, the emphasis on structural design has moved from the allowable stress design to the limit state design because the latter approach makes possible a rigorously designed, yet economical, structure that directly takes into consideration the various relevant modes of failure.

A limit state is formally defined by the description of a condition for which a particular structural member or an entire structure would fail to perform the function designated beforehand. From the viewpoint of structural design, four types of limit states are relevant for structures:

- The serviceability limit state (SLS)
- The ultimate limit state (ULS)
- The fatigue limit state (FLS)
- The accidental limit state (ALS)

The SLS represents failure states for normal operations due to deterioration from routine functioning. SLS considerations in design may address the following:

- Local damage that reduces the structure's durability or affects the efficiency of structural elements
- Unacceptable deformations that affect the efficient use of structural elements or the functioning of equipment that relies on them
- Excessive vibration or noise that can cause discomfort to people or affect the proper functioning of equipment
- Deformations and deflections that may spoil the structure's aesthetic appearance

The ULS (also called ultimate strength) represents the collapse of the structure due to a loss of structural stiffness and strength. Such loss of capacity may be related to:

- A loss of equilibrium, of a part or of the entire structure, which is often considered as a rigid body (e.g., overturning or capsizing)
- Attainment of the maximum resistance of structural regions, members, or connections by gross yielding or fracture
- Instability, of a part or of the entire structure, from buckling and plastic collapse of plating, stiffened panels, and support members

The FLS represents the occurrence of fatigue cracking of structural details due to stress concentration and damage accumulation or crack growth under repeated loading.

The ALS represents excessive structural damage from accidents, such as collisions, grounding, explosion, and fire, that affect the safety of the structure, the environment, and personnel.

The partial safety factor-based criterion of the limit state design for a particular type of limit state is typically given from Equation (1.11) as follows:

$$C_d > D_d \quad \text{or} \quad \frac{C_k}{\gamma_C} > \gamma_D D_k \tag{1.17}$$

It is important to emphasize that in the limit state design, these various types of limit states may be designed against different safety levels, with the actual safety level to be attained for a particular type of limit state being an indirect and implicit function of its perceived consequences and the ease of recovery from that state to be incorporated in design. Within the context of Equation (1.17), useful guidelines for determination of the partial safety factors related to a structure's limit state design may be found in ECCS (1982), BS 5950 (1985), ENV 1993-1 (1992a, 1992b), ISO 2394 (1998), and NORSOK (2004), among others.

1.2.1 Serviceability Limit State Design

The structural design criteria used for the SLS design of structures are normally based on the limits of deflections or vibration for normal use. In reality, the excessive deformation of a structure may also be associated with excessive vibration or noise, and thus certain interrelationships may exist among the design criteria being defined and used separately for convenience.

The SLS criteria are normally defined by the operator of a structure or by established practice, with the primary aim being efficient and economical in-service performance without excessive routine maintenance or downtime. The acceptable limits necessarily depend on the type, mission, and arrangement of structures. Furthermore, in defining such limits, experts in other disciplines, such as machinery design, must also be consulted. As an example, the limiting values of vertical deflections for beams in structures as shown in Figure 1.3 are indicated in Table 1.1.

In Table 1.1, L is the span of the beam between supports. For cantilever beams, L may be taken as twice the projecting length of the cantilever. δ_{max} is the maximum deflection, which is given by $\delta_{max} = \delta_1 + \delta_2 - \delta_0$, where δ_0 is the pre-camber, δ_1 is the variation of the deflection of the beam due to permanent loads immediately after loading, and δ_2 is the variation of the deflection of the beam due to variable loading plus any subsequent variant deflections due to permanent loads.

For plate elements, criteria based on elastic buckling control are often used for SLS design, in some cases to prevent such an occurrence entirely and in other cases to allow

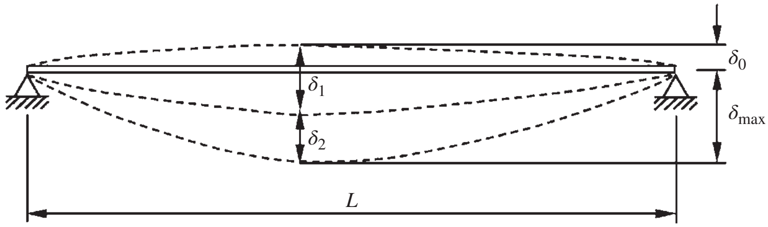

Figure 1.3 Nomenclature: lateral deflections of a beam.

Table 1.1 Serviceability limit values for vertical deflections of beams.

Condition	Limit for δ_{max}	Limit for δ_2
Deck beams	$L/200$	$L/300$
Deck beams that support plaster or other brittle finish or non-flexible partitions	$L/250$	$L/350$

elastic buckling to a known and controlled degree. Elastic plate buckling and its related effects, such as relatively large lateral deflections, must be prevented if such effects are likely to be detrimental. However, because a plate may have some reserve strength beyond elastic buckling until its ultimate strength is reached, allowing elastic buckling in a controlled manner can in some cases lead to a more economical structure. In Chapters 3 and 5 of this book, the use of such elastic buckling strength-based SLS design methods for plates and stiffened panels is described.

1.2.2 Ultimate Limit State Design

The structural design criteria to prevent the ULS are based on plastic collapse or ultimate strength. The simplified ULS design of many types of structures has tended to rely on estimates of the buckling strength of the components, usually from their elastic buckling strength adjusted by a simple plasticity correction, which is represented by point A in Figure 1.4. In such a design scheme based on the strength at point A, the structural designer does not use detailed information on the post-buckling behavior of the component members and their interactions. The true ultimate strength represented by point B in Figure 1.4 may be higher, although one can never be sure of this because the actual ultimate strength is not being directly evaluated.

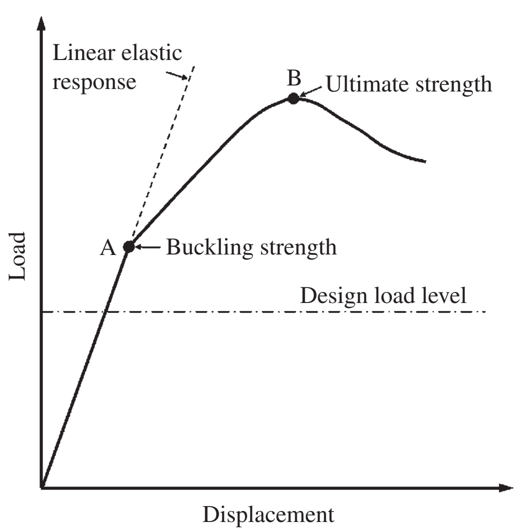

Figure 1.4 Structural design considerations based on the ultimate limit state.

In any event, as long as the strength level associated with point B remains unknown (as it is with traditional allowable stress design or linear elastic design methods), it is difficult to determine the real safety margin. Hence, more recently, the design of structures such as those of ships, offshore platforms, box girder bridges, and box girder cranes has tended to be based on the ultimate strength.

The safety margin of a structure can be evaluated by comparison of its ultimate strength with the extreme applied loads (or load effects, such as stress) as depicted in Figure 1.4. To obtain an economic yet safe structure, the ultimate strength and the design load must be assessed accurately. The structural designer may even desire to estimate the ultimate strength for not only the intact structure but also the structures with existing or in-service damage (e.g., corrosion wastage, fatigue cracking, or local denting damage) or even accident induced damage (e.g., due to collision, grounding, dropped object, fire, or explosion) to assess their damage tolerance and survivability.

The ULS design criterion can also be expressed by Equation (1.17). The characteristic measure of design capacity C_d in Equation (1.17) is in this case the ultimate strength, whereas D_d is the related load or demand measure. For ULS design, the partial safety factor γ_C is sometimes taken as $\gamma_C = 1.15$ for ships and offshore structures (NORSOK 2004).

It is important to note that any failure in a structure must ideally occur in a ductile manner rather than a brittle manner; the avoidance of brittle failure will lead to a structure that does not collapse suddenly, because ductility allows the structure to redistribute internal stresses and thus absorb greater amounts of energy before global failure. Adequate ductility in the design of a structure is facilitated by:

- Meeting the requisite material toughness requirements
- Avoiding failure initiation situations with a combination of high stress concentration and undetected weld defects in the structural details
- Designing structural details and connections to allow a certain amount of plastic deformation, that is, avoiding “hot spots”
- Arranging the members in such a manner that a sudden decrease in the structural capacity would not occur as a result of abrupt transitions or member failure

This book is primarily concerned with ULS design methods for structural members and systems composed of such ductile members, although other types of limit states are also described to some extent.

1.2.3 Fatigue Limit State Design

The FLS design is carried out to ensure that the structure has an adequate fatigue life. The predicted fatigue life can also be a basis for planning efficient inspection programs during the structure’s operation. The design fatigue life for structural components is normally based on the structure service life required by the operator or by other responsible body such as a class society. For ship structures, the fatigue life is often considered to be 25 years or longer. The shorter the design fatigue life, or the greater the required reliability, the smaller the inspection intervals should be to assure an operation free from crack problems.

The FLS design and analysis should in principle be undertaken for every suspected location of fatigue cracking, which includes welded joints and local areas of stress concentration.

The structural design criteria for the FLS are usually based on the structure's cumulative fatigue damage under repeated fluctuation of loading, as measured by the Palmgren–Miner cumulative damage rule. A particular value of the Miner sum (e.g., unity) is taken to be synonymous with the formation or initiation of a crack. The structure is designed so that when it is analyzed for fatigue, a reduced target Miner sum results, implying that cracks will not form with a given degree of certainty.

The fatigue damage at a crack initiation site is affected by many factors, such as the stress ranges experienced during load cycles, the local stress concentration characteristics, and the number of stress range cycles. Two types of the FLS design approach are typically considered for structures:

- The *S*–*N* curve approach (*S* = fluctuating stress, *N* = associated number of cycles)
- The fracture mechanics approach

In the *S*–*N* curve approach, the Palmgren–Miner cumulative damage rule is applied together with the relevant *S*–*N* curve. This application normally follows three steps: (i) definition of the histogram of cyclic stress ranges, (ii) selection of the relevant *S*–*N* curve, and (iii) calculation of the cumulative fatigue damage.

One of the most important factors in fatigue design is the characteristic stress to be used both in defining the *S*–*N* curve (the capacity) and in the stress analysis (with the fluctuating local fatigue stresses being the demand on the structure). Four types of methods have been suggested on this basis:

- The nominal stress method
- The hot spot stress method
- The notch stress method
- The notch strain method

The nominal stress method uses the nominal stresses in the field far from the stress concentration area, together with *S*–*N* curves that must include implicitly the effects of both structural geometry and the weld. In the nominal stress method, therefore, the *S*–*N* curve should be selected for structural details depending on the detail type and weld geometry involved. Many *S*–*N* curves for various types of weld and geometry are generally needed and are available. When a limited number of standard *S*–*N* curves are used, any structural detail considered must be assigned to one of those categories, which requires a certain amount of judgment.

The hot spot stress method uses a well-defined hot spot stress in the stress concentration area to account for the effect of structural geometry alone, and the weld effect is incorporated into the *S*–*N* curve. This is currently a very popular approach, but certain practical difficulties must be conceded. The most basic of these pertains to the concept of hot spot stress itself, which is more appropriate for surface cracks than for imbedded cracks. Difficulties can also arise in the consistent definition of hot spot stresses across a range of weld and structural geometries and in the estimation of the hot spot structural stress needed for application of the technology in regions of stress concentration. For instance, attention should be paid to extrapolation of the stress to the weld toe for calculation of the stress concentration factor, and the need for appropriate selection of a relevant *S*–*N* curve from those for different weld types is still significant.

The notch stress method uses the stresses at the notch calculated by accounting for the effects of both structural geometry and the weld, whereas the *S*–*N* curve is developed to represent the fatigue properties of either the base material, the material in the heat-affected zone (HAZ), or the weld material, as appropriate. A significant advantage of the notch stress method is that it can address the specific weld toe geometry in the calculation of fatigue damage. A related difficulty is that the relevant parameters (e.g., the weld toe angle) in the case of the actual structure must be known with some confidence.

The notch strain method uses the strains at the notch when the low-cycle fatigue is predominant, because the working stresses in this case sometimes likely approach the material yield stress, and thus the stress-based approaches are less appropriate.

The fracture mechanics approach considers that one or more premised cracks of a small dimension exist in the structure and predicts the fatigue damage during the process of crack propagation, including any coalescence and breakthrough, and the subsequent fracture. In this approach to design, a major task is to preestablish the relevant crack growth equations or "laws." The crack growth rate is often expressed as a function of only the stress intensity factor range at the crack tip, on the assumption that the yielded area around the crack tip is relatively small. In reality, the crack propagation behavior is affected by many other parameters (e.g., mean stresses, load sequence, crack retardation, crack closure, crack growth threshold, and stress intensity range) in addition to the stress intensity factor range.

The structural fracture mechanics is dealt with in Chapter 9, and the *S–N* curve approach using nominal stresses is herein briefly described under the assumption of the linear cumulative damage rule, that is, the Palmgren–Miner rule. In the fatigue damage assessment of welded structural details, of primary concern are the ranges of the cyclic maximum and minimum stresses rather than the mean stresses, as shown in Figure 1.5, because of the usual presence of residual mean stresses near the yield magnitude. This tends to make the entire stress range damaging. The situation in non-welded cases is, of course, different, and, in such cases, the mean stresses can be important.

For practical FLS design using the nominal stress-based approach, the relevant *S–N* curves must be developed for various types of weld joints. To do this, fatigue tests are carried out for various types of specimens that are subjected to cyclic stress ranges of a uniform amplitude. As indicated in Figure 1.5, the maximum and minimum stresses

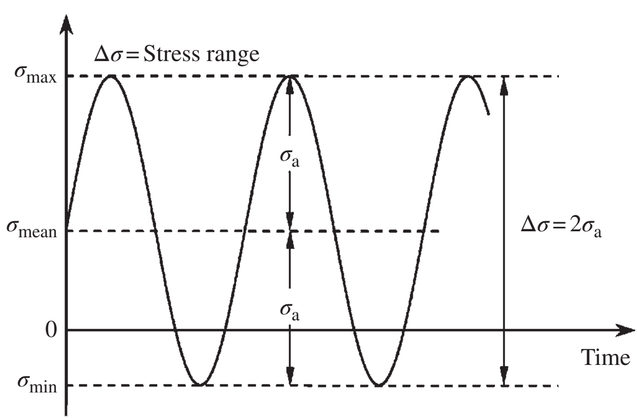

Figure 1.5 Cyclic stress range versus time.

are denoted by $\sigma_{\max}$ and $\sigma_{\min}$, respectively. In such tests, the effect of the mean stress, $\sigma_{\text{mean}} = (\sigma_{\max} + \sigma_{\min})/2$, on fatigue damage can be quantified, which is necessary for non-welded cases. For convenience, the fatigue tests for specimens that incorporate non-welded geometries are usually carried out at either $\sigma_{\min} = 0$ or $\sigma_{\max} = -\sigma_{\min}$ with a constant stress range, that is, $\Delta\sigma = \sigma_{\max} - \sigma_{\min} = 2\sigma_a$, where σ_a is the stress amplitude.

The number of stress cycles, N_I or N_F, with the former representing the crack initiation life, that is, until a crack initiates, and the latter representing the fracture life, such as until a small-scale test specimen is separated into two pieces, is obtained on the basis of the fatigue test results. With a series of such tests for a variety of stress ranges, $\Delta\sigma$, the *S–N* curves for the particular structural details may typically be plotted as shown in Figure 1.6. The curves for design are usually expressible by curve fitting the test results plotted on a log–log scale, namely,

$$\log N = \log a - 2s - m \log \Delta\sigma \tag{1.18a}$$

$$N(\Delta\sigma)^m = A \tag{1.18b}$$

where $\Delta\sigma$ is the stress range, N is the number of stress cycles with constant stress range, $\Delta\sigma$, until failure, m is the negative inverse slope of the *S–N* curve, $\log A = \log a - 2s$, a is the life intercept of the mean *S–N* curve, and s is the standard deviation of $\log N$.

For the FLS design criterion based on the *S–N* curve approach, Equation (1.17) may be rewritten in the nondimensional form when the distribution of a long-term stress range is given by a relevant stress histogram in terms of a number of constant amplitude stress range blocks, $\Delta\sigma_i$, each with a number of stress fluctuations, n_i, as follows:

$$D = \sum_{i=1}^{B} \frac{n_i}{N_i} = \frac{1}{A} \sum_{i=1}^{B} n_i (\Delta\sigma_i)^m \le D_{cr} \tag{1.19}$$

where D is the accumulated fatigue damage, B is the number of stress blocks, n_i is the number of stress cycles in stress block i, N_i is the number of cycles until failure at the ith constant amplitude stress range block, $\Delta\sigma_i$, and D_{cr} is the target cumulative fatigue damage for design.

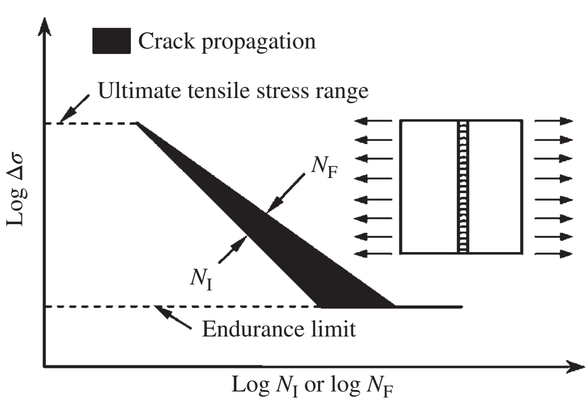

Figure 1.6 Typical *S–N* curves from constant amplitude tests.

To achieve greater fatigue durability in a structure, it is important to minimize stress concentrations, potential flaws (e.g., misalignment, poor materials), and structural degradation, including corrosion and fatigue effects. Fatigue design is interrelated with the maintenance regime to be used. In some cases, it may be more economical in design to allow the possibility of a certain level of fatigue damage, as long as the structure can continue to function after the fatigue symptoms are detected until repairs can be made. In other cases, fatigue damage may not be allowed to occur, if it is inconvenient to inspect the structure or interrupt production. The former approach may thus be applied as long as regular inspections and related maintenance are possible, whereas the latter concept is obviously more relevant if there are likely to be difficulties associated with inspections and thus a high likelihood of undetected fatigue damage.

Fatigue is sometimes classified into high-cycle fatigue and low-cycle fatigue. High-cycle fatigue indicates that a structure has a long fatigue life due to a small stress range, whereas low-cycle fatigue indicates that a structure has a short fatigue life due to a large stress range. The two are sometimes distinguished by the fatigue cycle of 10^4.

In Chapter 9, structural fracture mechanics and the ultimate strength of plate panels associated with fatigue cracking damage are described. For elaborate descriptions in fatigue damage analysis methods, interested readers may refer to Schijve (2009), Nussbaumer et al. (2011), and Lotsberg (2016), among others.

1.2.4 Accidental Limit State Design

The primary aim of the ALS design for structures may be characterized by the following three broad objectives:

- To avoid loss of life in the structure or the surrounding area
- To avoid pollution of the environment
- To minimize loss of property or financial exposure

In the ALS design, it is necessary to achieve a design in which the structure's main safety functions are not impaired during any accidental event or within a certain time after the accident. The structural design criteria for the ALS are based on limiting accidental consequences such as structural damage and environmental pollution.

Because the structural damage characteristics and behavior of damaged structures depend on the type of accidents, it is not straightforward to establish universally applicable structural design criteria for the ALS. Typically, for a given type of structure, the design of accidental scenarios and associated performance criteria must be decided on the basis of risk assessment.

In the case of ships or offshore platforms, possible accidental events that may need to be considered for the ALS include collisions, grounding, dropped objects, significant hydrodynamic impact (e.g., sloshing, slamming, or green water) that leads to buckling or structural damage, excessive loads from human error, berthing or dry docking, fires or internal gas explosions in oil tanks or machinery spaces, and underwater or atmospheric explosions. In land-based structures, the accidental scenarios may include fire, explosion, foundation movements, or related structural damage from earthquakes.

In selecting the design target ALS performance levels for such events, the approach is normally to tolerate a certain level of damage consistent with a greater aim such as survivability or minimized consequences; to do otherwise would result in an uneconomical structure.

The main safety functions of a structure that should not be compromised during any accident event or within a certain time after the accident include:

- Usability of escape ways
- Integrity of shelter areas and control spaces
- Global load-bearing capacity
- Integrity of the environment

Therefore, the ALS design criteria should be formulated so that the main safety functions mentioned previously will work successfully and the following points are considered to adequate levels:

- Energy dissipation related to structural crashworthiness
- Capacity of local strength members or structures
- Capacity of the global structure
- Allowable tensile strains to avoid tearing or rupture
- Endurance of fire protection

For the ALS design, the structure's integrity will typically be checked in two steps. In the first step, the structural performance will be assessed against design accident events, and post-accident effects such as damage to the environment are evaluated in the second step.

In the case of accidents to ships, for instance, the primary concern of the ALS design is to maintain the watertightness of the ship's compartments, the containment of dangerous or pollutant cargoes (e.g., chemicals, bulk oil, liquefied gas), and the integrity of the reactor compartments of nuclear-powered ships. To continue normal operations for the structure's mission, it is also important to maintain the integrity and residual strength of damaged structures at a certain level immediately after the accident occurs.

The different types of accident events normally require different methods to analyze the structure's resistance. For the ALS design criteria under predominantly impact-oriented loading, Equation (1.17) may typically be rewritten using energy dissipation-related criteria adopted with the view that the safety of the structure or the environment is not lost:

$$E_k \gamma_k < \frac{E_a}{\gamma_a} \tag{1.20}$$

where E_k is the kinetic energy lost during the accident, E_a is the available energy absorption capability until critical damage occurs, and γ_k and γ_a are partial safety factors related to kinetic energy loss and energy absorption capability, respectively.

The structure's dissipated energy during the accident may usually be calculated by integrating the area below the load–displacement curve of the structure under accidental loading, as shown in Figure 1.7. In Chapter 10, an elaborate description for the structural impact mechanics and the residual ultimate strength of plate panels with accident induced damage such as local denting is presented.

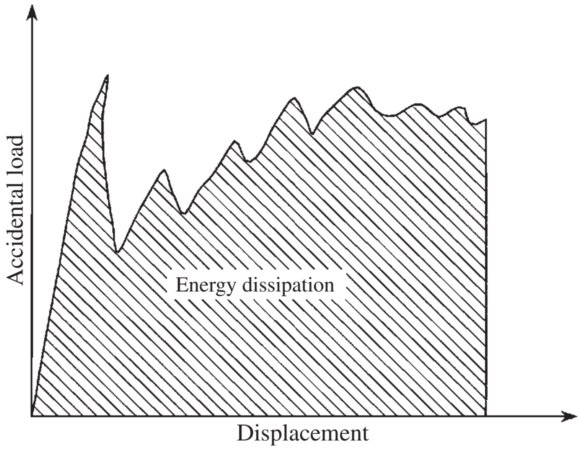

Figure 1.7 Energy absorption of the structure under accidental loading.

1.3 Mechanical Properties of Structural Materials

For materials of plated structures, steels or aluminum alloys are typically used. The specific gravity of aluminum alloys is about one-third that of steels, and thus aluminum alloys are primarily used in weight-critical structures. Aluminum alloys also have merits with their good resistance to corrosion by seawater and with an easier processing of extrusion, leading to the availability in a wide variety of section forms. However, the elastic modulus of aluminum alloys is only one-third that of steels, which is an apparent disadvantage of aluminum alloys.

In structural analysis and design, it is essential to define the material properties associated with the targeted structural systems. In industry practice, nominal values of material properties are often used in the analysis and design of a structure. When harsh environmental or operational conditions are of primary concern, however, the mechanical properties of the materials must be accurately quantified by considering the effects of such conditions. Because testing is only a method to quantify material properties, numerous test databases have been developed in the literature (e.g., Callister 1997); some are limited to specific conditions, and others are based on old materials that are no longer in use.

Modern material-manufacturing technologies have greatly advanced the material properties featured in old test databases, and today’s structural systems are often exposed to the harsher environmental and operational conditions associated with their functional requirements. Thus, test databases for these volatile material properties should be continuously developed to meet such requirements (Paik et al. 2017).

1.3.1 Characterization of Material Properties

The mechanical properties of structural materials are characterized by testing predesignated specimens under monotonic tensile loading. Figure 1.8 shows an idealized

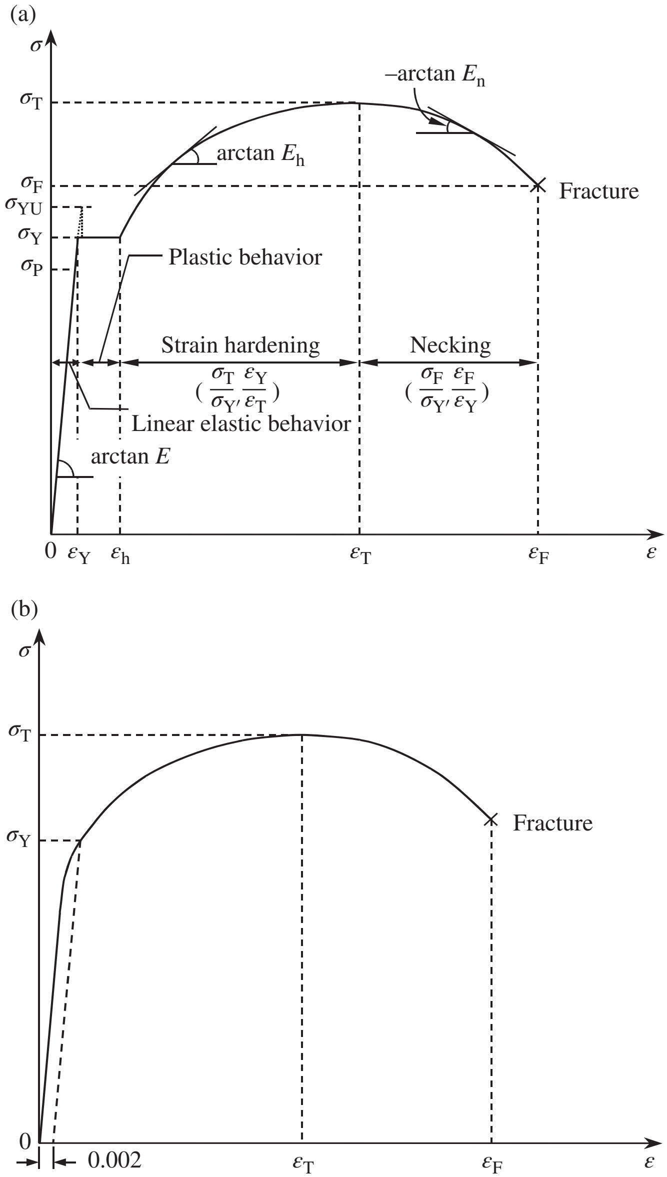

Figure 1.8 Schematic of engineering stress–engineering strain relationship for (a) ductile materials and (b) specially treated ductile materials.

engineering stress–engineering strain curve for structural metals. The material properties can be characterized using the following parameters:

- Young's modulus (or modulus of elasticity), E
- Poisson's ratio, ν
- Proportional limit, σ_P

- Upper yield point, σ_{YU}
- Lower yield point, σ_{YL} ($\approx\sigma_Y$)
- Yield strength, σ_Y
- Yield strain, ε_Y
- Strain-hardening strain, ε_h
- Strain-hardening tangent modulus, E_h
- Ultimate tensile strength, σ_T
- Ultimate tensile strain, ε_T
- Necking tangent modulus, E_n
- Necking stress at fracture (total breaking), σ_F
- Fracture (total breaking) strain, ε_F

1.3.1.1 Young's Modulus, *E*

The initial relationship between stress and strain is linear elastic, wherein the material recovers perfectly upon unloading. The slope of the linear portion of the stress–strain relationship in the elastic regime is defined as the modulus of elasticity, E (also called Young's modulus). Table 1.2 indicates typical values of Young's moduli for selected metals and metal alloys at room temperature. Young's modulus of aluminum alloys is about one-third that of steel.

1.3.1.2 Poisson's Ratio, *v*

Poisson's ratio is defined as the ratio of the transverse strain to the longitudinal strain of a material under tensile load in the elastic regime. Table 1.2 indicates typical values of Poisson's ratio for selected metals and metal alloys at room temperature.

1.3.1.3 Elastic Shear Modulus, *G*

The mechanical properties of materials under shear are usually defined using principles of structural mechanics rather than by testing. The elastic shear modulus is expressed by a function of Young's modulus, E, and Poisson's ratio, ν, as follows:

$$G = \frac{E}{2(1+\nu)} \tag{1.21}$$

Table 1.2 Typical values of Young's moduli and Poisson's ratios for selected metals and metal alloys at room temperature.

Material	E (GPa)	ν
Aluminum alloy	70	0.33
Copper	110	0.34
Steel	205.8	0.3
Titanium	104–116	0.34

1.3.1.4 Proportional Limit, σ_P

The maximum stress in the elastic regime, that is, immediately before initial yielding, is termed the proportional limit, σ_P.

1.3.1.5 Yield Strength, σ_Y, and Yield Strain, ε_Y

Strictly speaking, structural materials without special treatment (e.g., quenching, tempering) may have upper and lower yield points, as illustrated in Figure 1.8a. The lower yield point typically has an extended plateau in the stress–strain curve, which is approximated by the yield strength σ_Y and the corresponding yield strain, $\varepsilon_Y = \sigma_Y/E$.

The mechanical properties of structural materials vary with the amount of work and heat treatment applied during the rolling process. Typically, plates that receive more work have a higher yield strength than plates that do not. The yield strength of metals is usually increased by special treatment.

Figure 1.8b illustrates an idealized engineering stress–engineering strain curve of specially treated metals or metal alloys in which neither upper nor lower yield points appear until the ultimate tensile strength is reached. In this case, the yield strength is commonly defined as the stress at the intersection of the stress–strain curve and a straight line through an offset point strain, $(\sigma,\varepsilon) = (0, 0.002)$, that is, the proof stress at 0.2% strain, that is, with $\varepsilon = 0.002$, which is parallel to the linear portion of the stress–strain curve in the elastic regime.

It is important to realize that a material's yield strength is significantly affected by operational and environmental conditions, such as temperatures and loading speed (or strain rates), among others. For structural design purposes, regulatory bodies or classification societies identify the "minimum" requirements for the mechanical properties and the chemical composition of materials. For example, the International Association of Classification Societies (IACS) specify the minimum requirements of the yield strength, ultimate tensile strength, and fracture strain (elongation) of rolled or extruded aluminum alloys for marine applications, as indicated in Tables 1.3 and 1.4 (IACS 2014). Interested readers may also refer to Sielski (2007, 2008).

1.3.1.6 Strain-Hardening Tangent Modulus, E_h, and Strain-Hardening Strain, ε_h

Beyond the yield stress or strain, the metal flows plastically without appreciable changes in stress until the strain-hardening strain ε_h is reached. The slope of the stress–strain curve in the strain-hardening regime is defined as the strain-hardening tangent modulus E_h, which may not be constant, but rather dependent on different conditions.

Strain hardening may also be characterized as the ratio of the ultimate tensile stress σ_T to the yield stress σ_Y or as the ratio of the ultimate tensile stress ε_T to the yield strain ε_Y. The stress σ beyond the yield strength of the elastic–plastic material with strain hardening is often expressed at a certain level of plastic strain as follows:

$$\sigma = \sigma_Y + \frac{EE_h}{E - E_h}\varepsilon_p \tag{1.22}$$

where ε_p is the effective plastic strain.

1.3.1.7 Ultimate Tensile Strength, σ_T

When strain exceeds the strain-hardening strain, ε_h, the stress increases above the yield stress, σ_Y, because of strain hardening, and this behavior can continue until the ultimate

Table 1.3 Minimum requirements of the mechanical properties for rolled aluminum alloys (IACS 2014).

Grade	Temper	Thickness t (mm)	σ_Y (MPa)	σ_T (MPa)	ε_F (%)	
					$t \le 12.5$ mm	$t > 12.5$ mm
5083	O	$3 \le t \le 50$	125	275–350	16	14
	H111	$3 \le t \le 50$	125	275–350	16	14
	H112	$3 \le t \le 50$	125	275	12	10
	H116	$3 \le t \le 50$	215	305	10	10
	H321	$3 \le t \le 50$	215–295	305–385	12	10
5383	O	$3 \le t \le 50$	145	290	–	17
	H111	$3 \le t \le 50$	145	290	–	17
	H116	$3 \le t \le 50$	220	305	10	10
	H321	$3 \le t \le 50$	220	305	10	10
5059	O	$3 \le t \le 50$	160	330	24	24
	H111	$3 \le t \le 50$	160	330	24	24
	H116	$3 \le t \le 20$	270	370	10	10
		$20 < t \le 50$	260	360	–	10
	H321	$3 \le t \le 20$	270	370	10	10
		$20 < t \le 50$	260	360	–	10
5086	O	$3 \le t \le 50$	95	240–305	16	14
	H111	$3 \le t \le 50$	95	240–305	16	14
	H112	$3 \le t \le 12.5$	125	250	8	–
		$12.5 < t \le 50$	105	240	–	9
	H116	$3 \le t \le 50$	195	275	10[1)]	9
5754	O	$3 \le t \le 50$	80	190–240	18	17
	H111	$3 \le t \le 50$	80	190–240	18	17
5456	O	$3 \le t \le 6.3$	130–205	290–365	16	–
		$6.3 < t \le 50$	125–205	285–360	16	14
	H116	$3 \le t \le 30$	230	315	10	10
		$30 < t \le 40$	215	305	–	10
		$40 < t \le 50$	200	285	–	10
	H321	$3 \le t \le 12.5$	230–315	315–405	12	–
		$12.5 < t \le 40$	215–305	305–385	–	10
		$40 < t \le 50$	200–295	285–370	–	10

Notes:

a) 8% for $t \le 6.3$ mm.

b) The mechanical properties for the O and H111 tempers are the same, but they are separated to encourage dual certification as these tempers represent different processing.

Table 1.4 Minimum requirements of the mechanical properties for extruded aluminum alloys (IACS 2014).

Grade	Temper	Thickness t (mm)	σ_Y (MPa)	σ_T (MPa)	ε_F (%)	
					$t \le 12.5$mm	$t > 12.5$mm
5083	O	$3 \le t \le 50$	110	270–350	14	12
	H111	$3 \le t \le 50$	165	275	12	10
	H112	$3 \le t \le 50$	110	270	12	10
5383	O	$3 \le t \le 50$	145	290	17	17
	H111	$3 \le t \le 50$	145	290	17	17
	H112	$3 \le t \le 50$	190	310	–	13
5059	H112	$3 \le t \le 50$	200	330	–	10
5086	O	$3 \le t \le 50$	95	240–315	14	12
	H111	$3 \le t \le 50$	145	250	12	10
	H112	$3 \le t \le 50$	95	240	12	10
6005A	T5	$3 \le t \le 50$	215	260	9	8
	T6	$3 \le t \le 10$	215	260	8	6
		$10 < t \le 50$	200	250	8	6
6061	T6	$3 \le t \le 50$	240	260	10	8
6082	T5	$3 \le t \le 50$	230	270	8	6
	T6	$3 \le t \le 5$	250	290	6	–
		$5 < t \le 50$	260	310	10	–

tensile strength (also simply termed tensile strength), σ_T, is reached. The value of σ_T is obtained by the maximum axial tensile load divided by the original cross-sectional area of the test specimen. Tables 1.3 and 1.4 indicate the minimum requirements of the ultimate tensile strength for rolled or extruded aluminum alloys.

1.3.1.8 Necking Tangent Modulus, E_n

With further increase in strain, a large local reduction of the cross section occurs, which is termed necking or strain softening. The internal engineering stress decreases in the necking regime. The slope of the engineering stress–engineering strain curve in the necking regime is sometimes defined as the necking tangent modulus, E_n. Necking may also be characterized as the ratio of the fracture stress σ_F to the ultimate tensile stress σ_T or as the ratio of the fracture strain ε_F to the ultimate tensile strain ε_T.

1.3.1.9 Fracture Strain, ε_F, and Fracture Stress, σ_F

Fracture takes place when the strain reaches the fracture strain (elongation or total breaking strain), ε_F. The fracture stress σ_F is defined as the stress at fracture in the necking regime. Fracture strain is also significantly affected by operational and environmental conditions, such as temperatures and loading speed (or strain rates), among other factors.

Tables 1.3 and 1.4 indicate the minimum requirements of the fracture strain for rolled or extruded aluminum alloys.

1.3.2 Elastic–Perfectly Plastic Material Model

Figure 1.9 shows the illustrative effects of strain hardening on the elastic–plastic large-deflection behavior (i.e., average stress–average strain curve) of a steel rectangular plate under uniaxial compressive loads in the longitudinal direction, as obtained by the nonlinear finite element analysis. The characteristics of the strain hardening are varied as shown in Figure 1.9a in the analysis. The plate is simply supported at all four edges, keeping them straight. It is evident that the strain-hardening effect can cause the plate ultimate strength to be greater than that obtained by neglecting it.

For the ULS assessment of structures made of ductile materials, an elastic–perfectly plastic material model, as shown in Figure 1.10, that is, one without strain hardening or necking, is often applied because strains are usually not significant. This material model may lead to a pessimistic estimation of the characteristic value of capacity. For the ALS assessment, however, the true stress–true strain relation with strain-hardening and necking effects should be considered because large plastic strains are usually involved.

1.3.3 Characterization of the Engineering Stress–Engineering Strain Relationship

When the details of the relationship between engineering stress σ versus engineering strain ε are unavailable, but such fundamental parameters as the elastic modulus E and the yield strength σ_Y are known, the relationship between engineering stress and engineering strain can often be approximated using the Ramberg–Osgood equation, which was originally proposed for aluminum alloys (Ramberg & Osgood 1943), as follows:

$$\varepsilon = \frac{\sigma}{E} + \left(\frac{\sigma}{B}\right)^n \tag{1.23}$$

where E is the elastic modulus at the origin of the stress versus strain curve, ε is the engineering strain, σ is the engineering stress, and B and n are constants to be determined by experiments.

Equation (1.23) is often simplified as follows (Mazzolani 1985):

$$\varepsilon = \frac{\sigma}{E} + 0.002\left(\frac{\sigma}{\sigma_{0.2}}\right)^n \tag{1.24a}$$

where $\sigma_{0.2}$ is the proof stress at 0.2% strain, that is, with $\varepsilon = 0.002$, which is usually taken as material yield stress σ_Y, that is, $\sigma_{0.2} = \sigma_Y$, as shown in Figure 1.11. Exponent n is given as a function of $\sigma_{0.2}$ and $\sigma_{0.1}$ as follows:

$$n = \frac{\ln 2}{\ln(\sigma_{0.2}/\sigma_{0.1})} \tag{1.24b}$$

where $\sigma_{0.1}$ is the proof stress at 0.1% strain, with $\varepsilon = 0.001$.

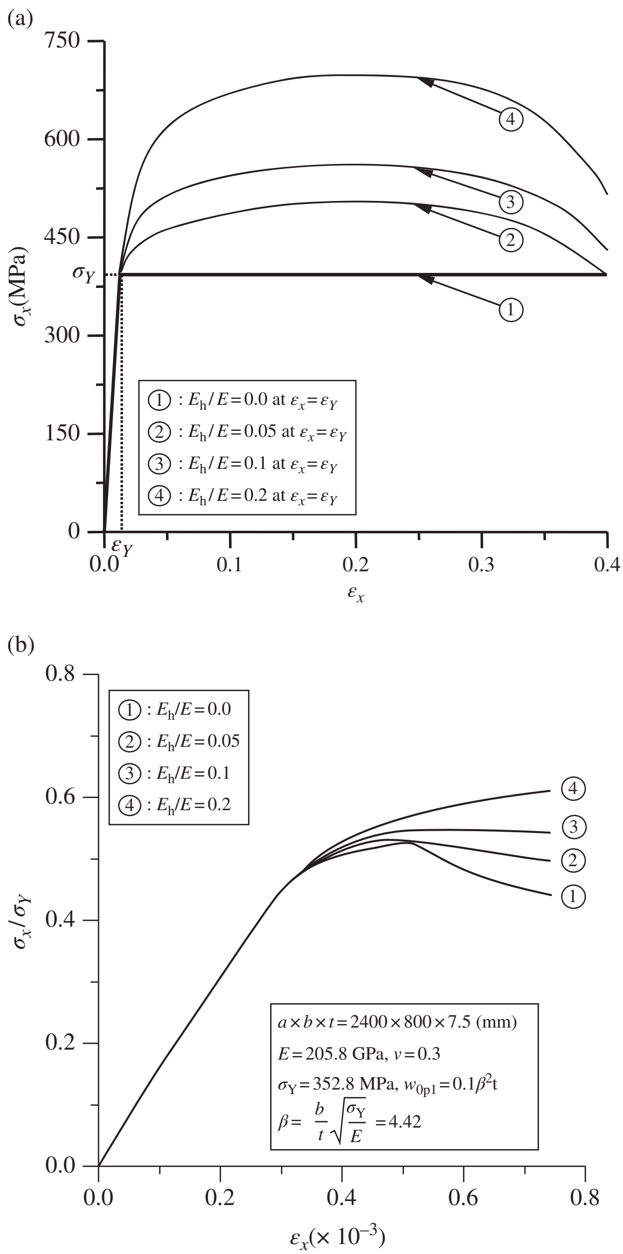

Figure 1.9 The effect of strain hardening on the ultimate strength of a steel plate under axial compression: (a) the engineering stress–engineering strain curves varying the strain-hardening characteristics; (b) a thin plate; (c) a thick plate (w_{0pl}, buckling mode initial deflection of the plate).

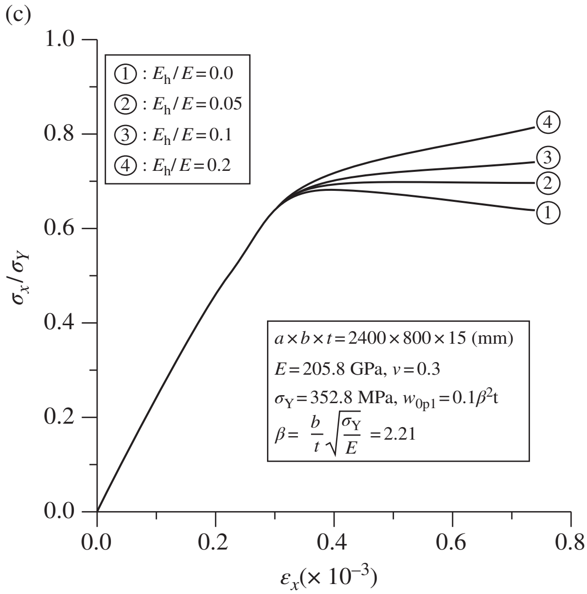

Figure 1.9 (Continued)

When the Ramberg–Osgood law is used, one practical difficulty is the determination of $\sigma_{0.1}$, in addition to E and $\sigma_{0.2}$ ($\approx \sigma_Y$). Without considering the strain-hardening effect, if the ratio $\sigma_{0.2}/\sigma_{0.1}$ approaches 1 (or $\sigma_{0.1} = \sigma_{0.2}$), the exponent becomes infinity, that is, $n = \infty$. This behavior corresponds to the elastic–perfectly plastic model of material, as illustrated in Figure 1.10, which can be expressed by

$$\varepsilon = \frac{\sigma}{E} + 0.002\left(\frac{\sigma}{\sigma_{0.2}}\right)^{\infty} \tag{1.25}$$

For aluminum alloys, Steinhardt (1971) proposed an approximate method for determining exponent n without the value of $\sigma_{0.1}$ being known as follows:

$$0.1n = \sigma_{0.2}\left(\mathrm{N/mm^2}\right) \quad \text{or} \quad n = 10\sigma_{0.2} \tag{1.26}$$

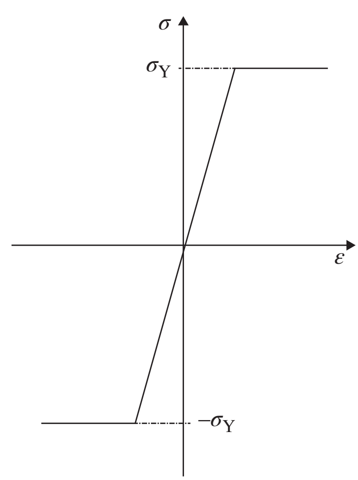

Figure 1.10 The elastic–perfectly plastic model of material.

1.3.4 Characterization of the True Stress–True Strain Relationship

For structural materials, the engineering stress–engineering strain relationship can be converted to the true stress–true strain relationship as follows:

$$\sigma_{\text{true}} = \sigma(1+\varepsilon), \quad \varepsilon_{\text{true}} = \ln(1+\varepsilon) \tag{1.27}$$

where σ_{true} is the true stress, $\varepsilon_{\text{true}}$ is the true strain, σ is the engineering stress, and ε is the engineering strain.

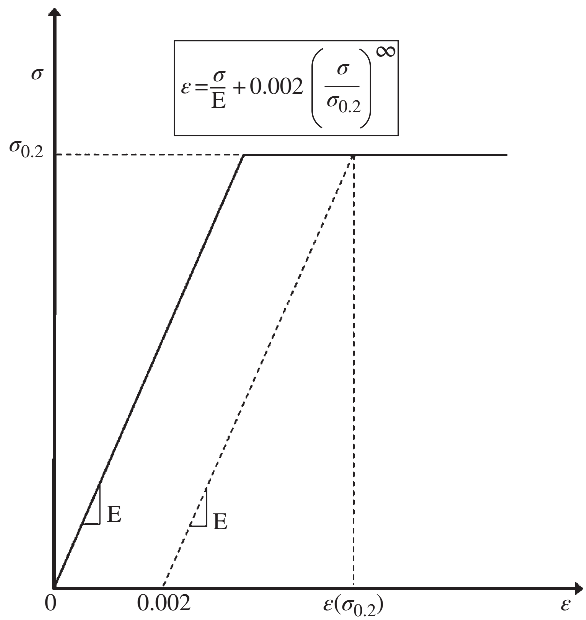

Figure 1.11 The Ramberg–Osgood law with the elastic–perfectly plastic model of material.

Figure 1.12 shows the engineering stress–engineering strain curve versus the true stress–true strain curve for mild steel and the aluminum alloy 5383-H116. It is recognized that Equation (1.27) tends to overestimate the strain-hardening and necking (strain-softening) effects. To resolve this issue, Paik (2007a, 2007b) suggested that Equation (1.27) be modified by the introduction of a knockdown factor that is a function of the engineering strain as follows:

$$\sigma_{\text{true}} = f(\varepsilon)\sigma(1+\varepsilon), \quad \varepsilon_{\text{true}} = \ln(1+\varepsilon) \tag{1.28a}$$

$$f(\varepsilon) = \begin{cases} \dfrac{C_1 - 1}{\ln(1+\varepsilon_T)}\ln(1+\varepsilon) + 1 & \text{for } 0 < \varepsilon \le \varepsilon_T \\ \dfrac{C_2 - C_1}{\ln(1+\varepsilon_F) - \ln(1+\varepsilon_T)}\ln(1+\varepsilon) + C_1 - \dfrac{(C_2 - C_1)\ln(1+\varepsilon_T)}{\ln(1+\varepsilon_F) - \ln(1+\varepsilon_T)} & \text{for } \varepsilon_T < \varepsilon \le \varepsilon_F \end{cases} \tag{1.28b}$$

where $f(\varepsilon)$ is the knockdown factor as a function of the engineering strain, ε_F is the material's fracture strain (elongation), ε_T is the strain at the ultimate tensile stress, and C_1 and C_2 are the test constants affected by material type and plate thickness, among other factors.

Although the knockdown factor is governed by the characteristics of the material type and plate thickness, the test constants may be given as $C_1 = 0.9$ and $C_2 = 0.85$ for mild and high-tensile steel (Paik 2007a, 2007b). Figure 1.13 compares the original true stress–true strain curve versus the modified (knocked-down) true stress–true strain curve of mild steel and the aluminum alloy 5383-H116, where the constants $C_1 = 0.9$ and $C_2 = 0.85$ are applied for both mild steel and the aluminum alloy.

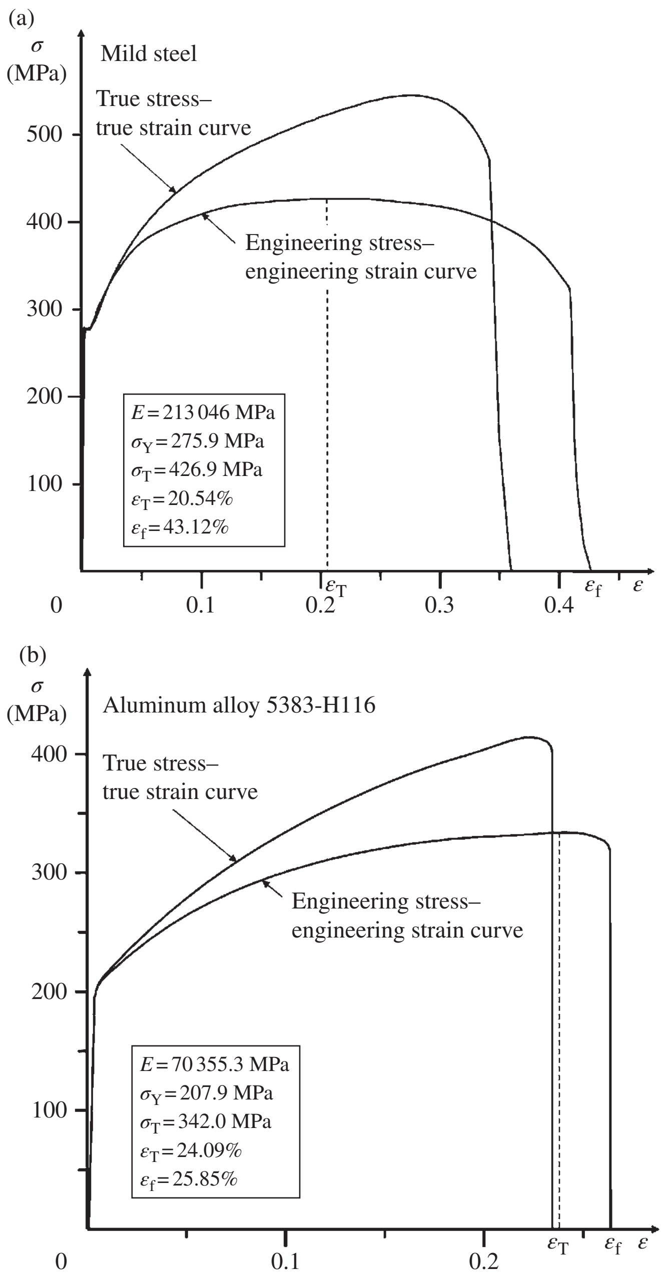

Figure 1.12 Engineering stress–engineering strain curve versus true stress–true strain curve for materials: (a) mild steel; (b) aluminum alloy 5383-H116.

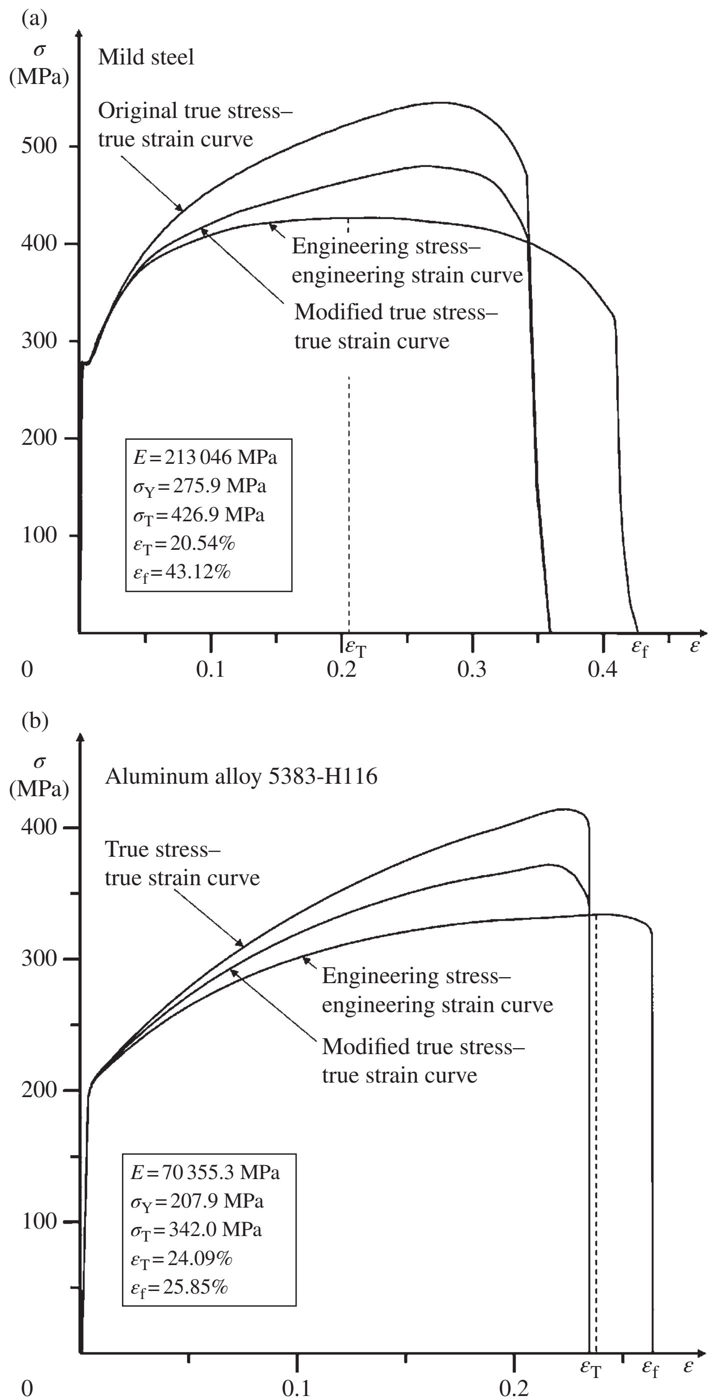

Figure 1.13 The original true stress–true strain curve versus the modified true stress–true strain curve for materials: (a) mild steel; (b) aluminum alloy 5383-H116.

1.3.5 Effect of Strain Rates

A material's mechanical properties are significantly affected by loading speed or strain rates $\dot{\varepsilon}$, which can be determined in an approximate fashion by assuming that the initial speed V_0 of the dynamic loads is linearly reduced to zero until the loading is finished, with average displacement δ, namely,

$$\dot{\varepsilon} = \frac{V_0}{2\delta} \tag{1.29}$$

In structural crashworthiness and/or impact response analysis, strain rate sensitivity plays an important role. Therefore, material modeling in terms of the dynamic yield strength and dynamic fracture strain must be considered. Figure 1.14 shows the engineering stress–engineering strain curves with varying strain rates obtained from experiments with mild steel (Grade A) and aluminum alloy 5083-O at room temperature, respectively (Paik et al. 2017).

As described in Section 10.3.2, the dynamic yield strength is often determined from the following Cowper–Symonds equation (Cowper & Symonds 1957):

$$\sigma_{\mathrm{Yd}} = \left\{1 + \left(\frac{\dot{\varepsilon}}{C}\right)^{1/q}\right\}\sigma_{\mathrm{Y}} \tag{1.30a}$$

where σ_{Y} is the static yield stress, σ_{Yd} is the dynamic yield stress, $\dot{\varepsilon}$ is the strain rate (1/s), and C and q are test constants, which may be taken as $C = 40.4/\mathrm{s}$, $q = 5$ for mild steel, $C = 3200/\mathrm{s}$, $q = 5$ for high-tensile steel, and $C = 6500/\mathrm{s}$, $q = 4$ for aluminum alloys (Paik & Thayamballi 2007, Jones 2012, Paik et al. 2017).

The dynamic fracture strain is taken as the inverse of the Cowper–Symonds equation for the dynamic yield strength as follows:

$$\varepsilon_{\mathrm{Fd}} = \left\{1 + \left(\frac{\dot{\varepsilon}}{C}\right)^{1/q}\right\}^{-1}\varepsilon_{\mathrm{F}} \tag{1.30b}$$

where ε_{F} is the static fracture strain and $\varepsilon_{\mathrm{Fd}}$ is the dynamic fracture strain. It is noted that the test constants C and q for the dynamic fracture strain are different from those for the dynamic yield strength as described in Section 10.3.3.

Figures 1.15 and 1.16 show the effects of strain rates combined with cold temperatures on the yield strength or fracture strain obtained from experiments for mild steel, high-tensile steel, and aluminum alloy 5083-O, obtained from the experiments by Paik et al. (2017).

1.3.6 Effect of Elevated Temperatures

A material's mechanical properties are significantly decreased with elevated temperatures from operational and environmental conditions or accidents such as fires because the material's properties are associated with its thermal characteristics. Figure 1.17a shows the specific heat of steel, which varies with elevated temperature. The reduction factors of the proportional limit, Young's modulus, and yield strength for steel are indicated in Table 1.5 according to the ECCS Eurocode design manuals (Franssen & Real 2010).

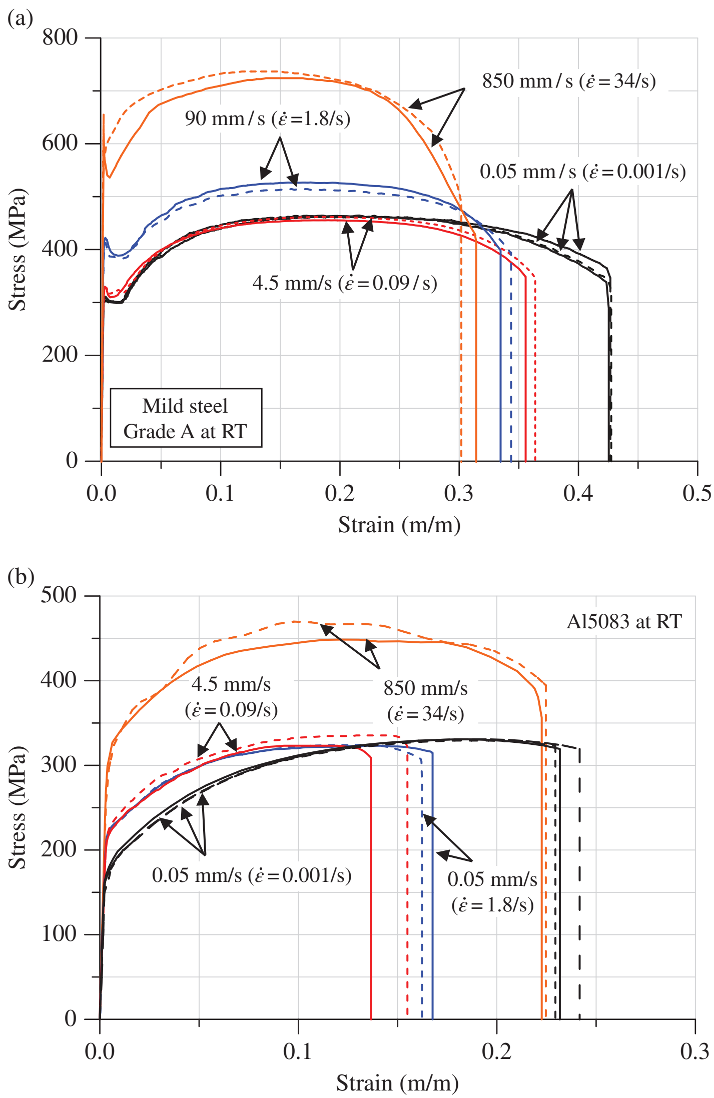

Figure 1.14 Engineering stress–engineering strain curves with different strain rates at room temperature (RT): (a) for mild steel (Grade A); (b) aluminum alloy 5083-O (Paik et al. 2017).

Figure 1.17b plots Table 1.5, showing that the mechanical properties of steel significantly decrease at temperatures above 400°C.

1.3.7 Effect of Cold Temperatures

The mechanical properties of materials are significantly affected by cold temperatures, which may be caused by operational conditions due to liquefied petroleum or natural gas

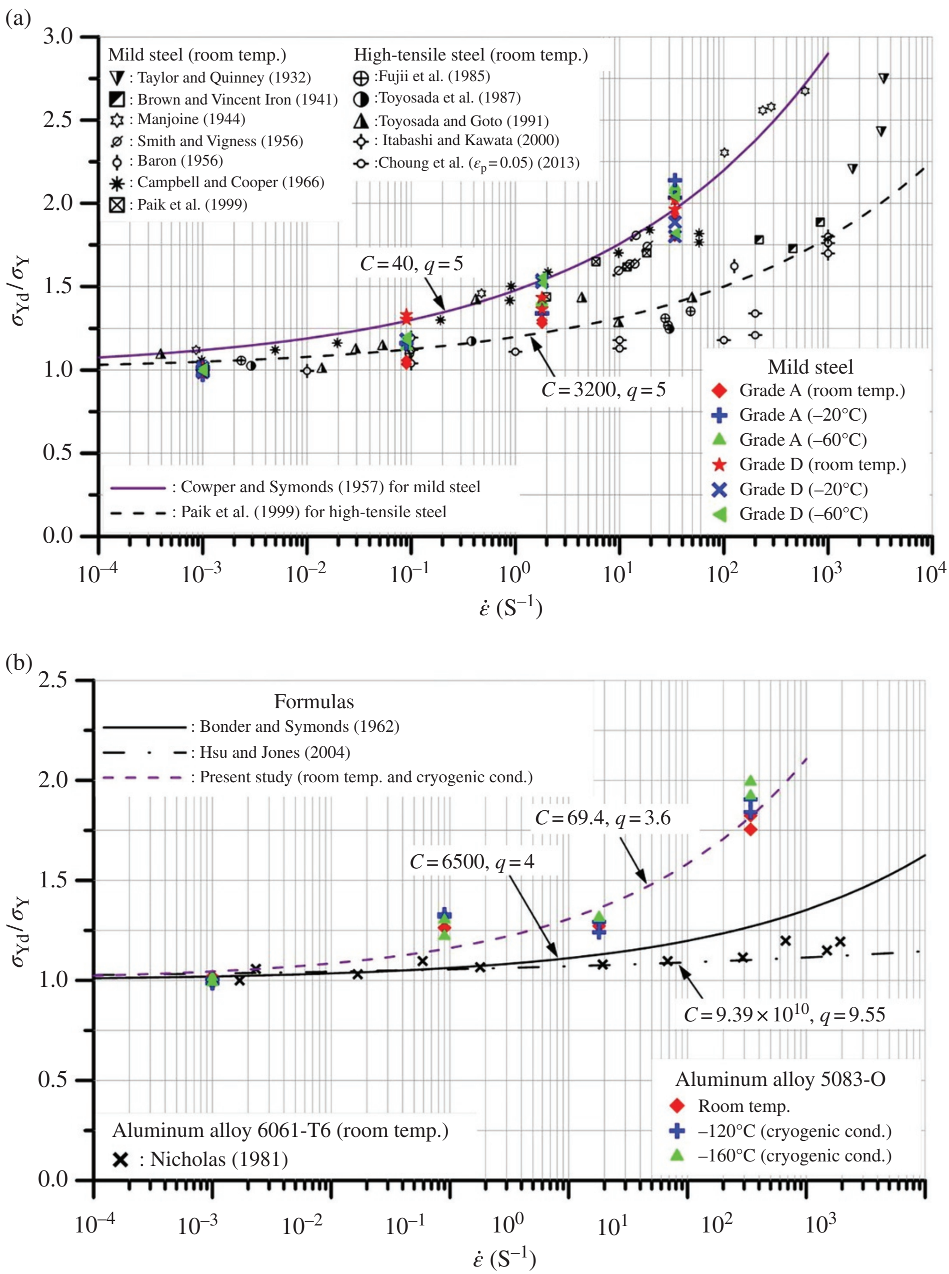

Figure 1.15 Effect of strain rates and cold temperatures on yield strength of materials: (a) mild steel and high-tensile steel; (b) aluminum alloy 5083-O. (Cited references are from Paik et al. 2017.)

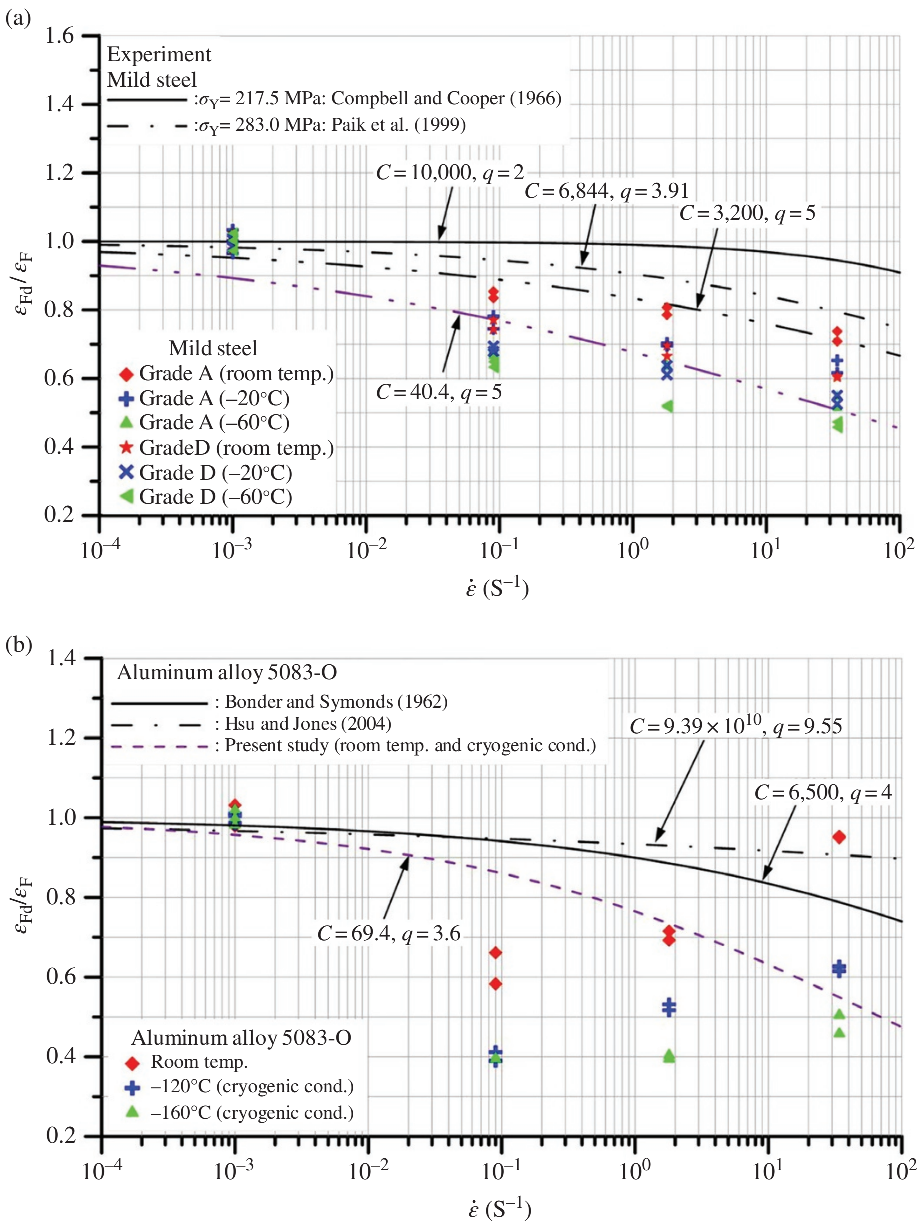

Figure 1.16 Effect of strain rates and cold temperatures on fracture strain of materials: (a) mild steel and high-tensile steel; (b) aluminum alloy 5083-O. (Cited references are from Paik et al. 2017.)

cargoes and by environmental conditions due to Arctic operations. Figures 1.18 and 1.19 show the combined effects of cold temperatures and strain rates on the yield strength or fracture strain of mild steel (Grade A) and aluminum alloy 5083-O, obtained from the experiments by Paik et al. (2017).

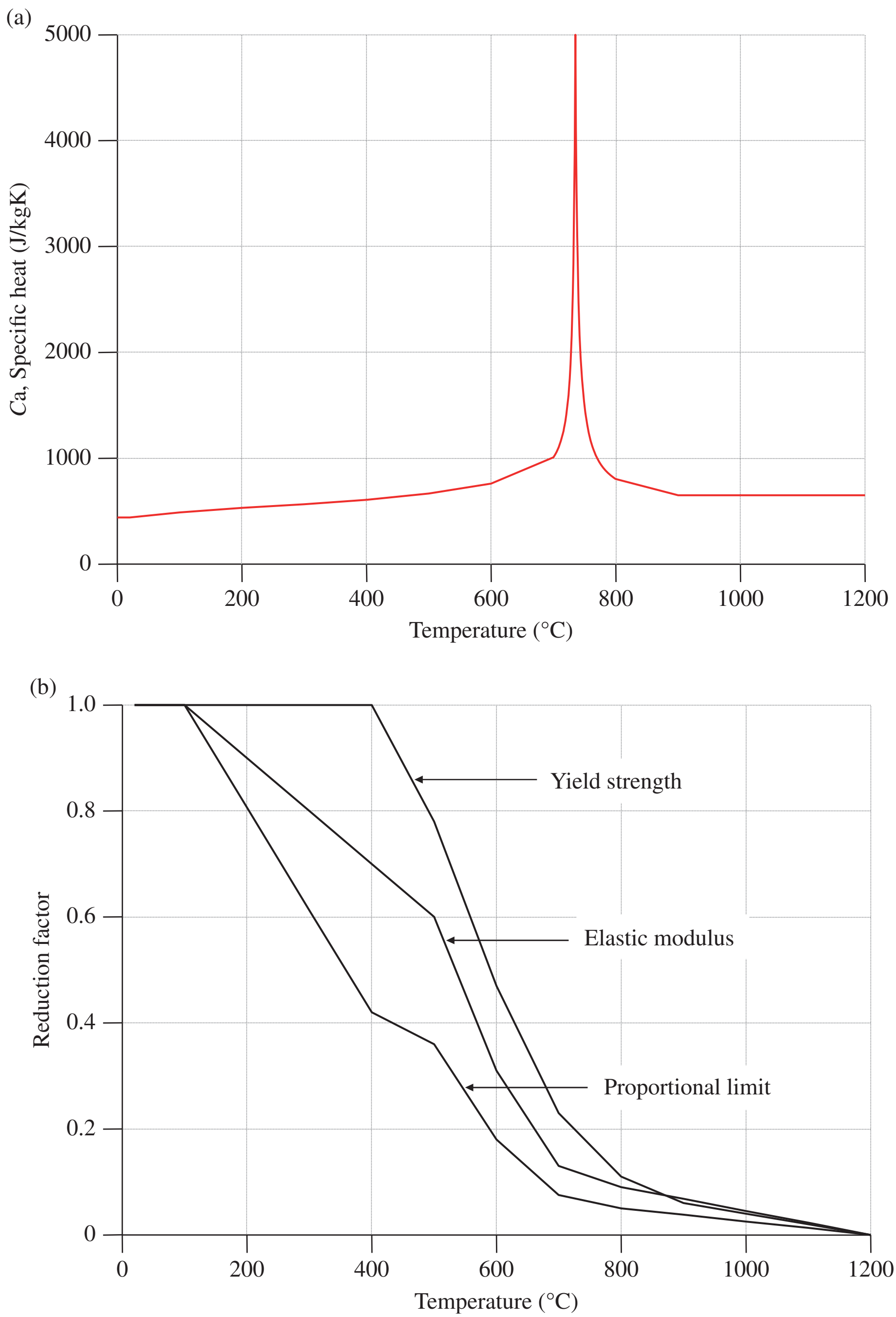

Figure 1.17 Effects of elevated temperature on properties of steel: (a) specific heat (ECCS 1982); (b) mechanical properties.

Table 1.5 Reduction factors of mechanical properties for carbon steels at elevated temperatures.

	Reduction factors at temperature relative to value of σ_Y, σ_P, or E at 20°C		
Steel temperature (°C)	σ_Y	σ_P	E
20	1.000	1.0000	1.0000
100	1.000	1.0000	1.0000
200	1.000	0.8070	0.9000
300	1.000	0.6130	0.8000
400	1.000	0.4200	0.7000
500	0.780	0.3600	0.6000
600	0.470	0.1800	0.3100
700	0.230	0.0750	0.1300
800	0.110	0.0505	0.0900
900	0.060	0.0375	0.0675
1000	0.040	0.0250	0.0450
1100	0.020	0.0125	0.0225
1200	0.000	0.0000	0.0000

Note: For intermediate values of the steel temperature, a linear interpolation may be used.

1.3.8 Yield Condition Under Multiple Stress Components

For a one-dimensional strength member under uniaxial tensile or compressive loading, the yield strength determined from a uniaxial tension test can be used to check the state of yielding, with the essential question to be answered being simply whether the axial stress reaches the yield strength.

A plate element that is the principal strength member of a steel- or aluminum-plated structure is likely to be subjected to a combination of biaxial tension/compression and shear stress, which can usually be considered to be in a plane stress state (as contrasted to a state of plane strain).

For an isotropic two-dimensional structural member for which the dimension in one direction is much smaller than those in the other two directions, and with three in-plane stress components (i.e., two normal stresses, σ_x, σ_y, and shear stress, τ_{xy}) or, equivalently, two principal stress components (i.e., σ_1, σ_2), three types of yield criteria are usually adopted as follows:

1) Maximum principal stress-based criterion: The material yields if the maximum absolute value of the two principal stresses reaches a critical value, namely,

$$\max(|\sigma_1|, |\sigma_2|) = \sigma_Y \tag{1.31a}$$

2) Maximum shear stress-based criterion (also called the Tresca criterion): The material yields if the maximum shear stress, τ_{max}, reaches a critical value, namely,

$$\tau_{max} = \left|\frac{\sigma_1 - \sigma_2}{2}\right| = \frac{\sigma_Y}{2} \tag{1.31b}$$

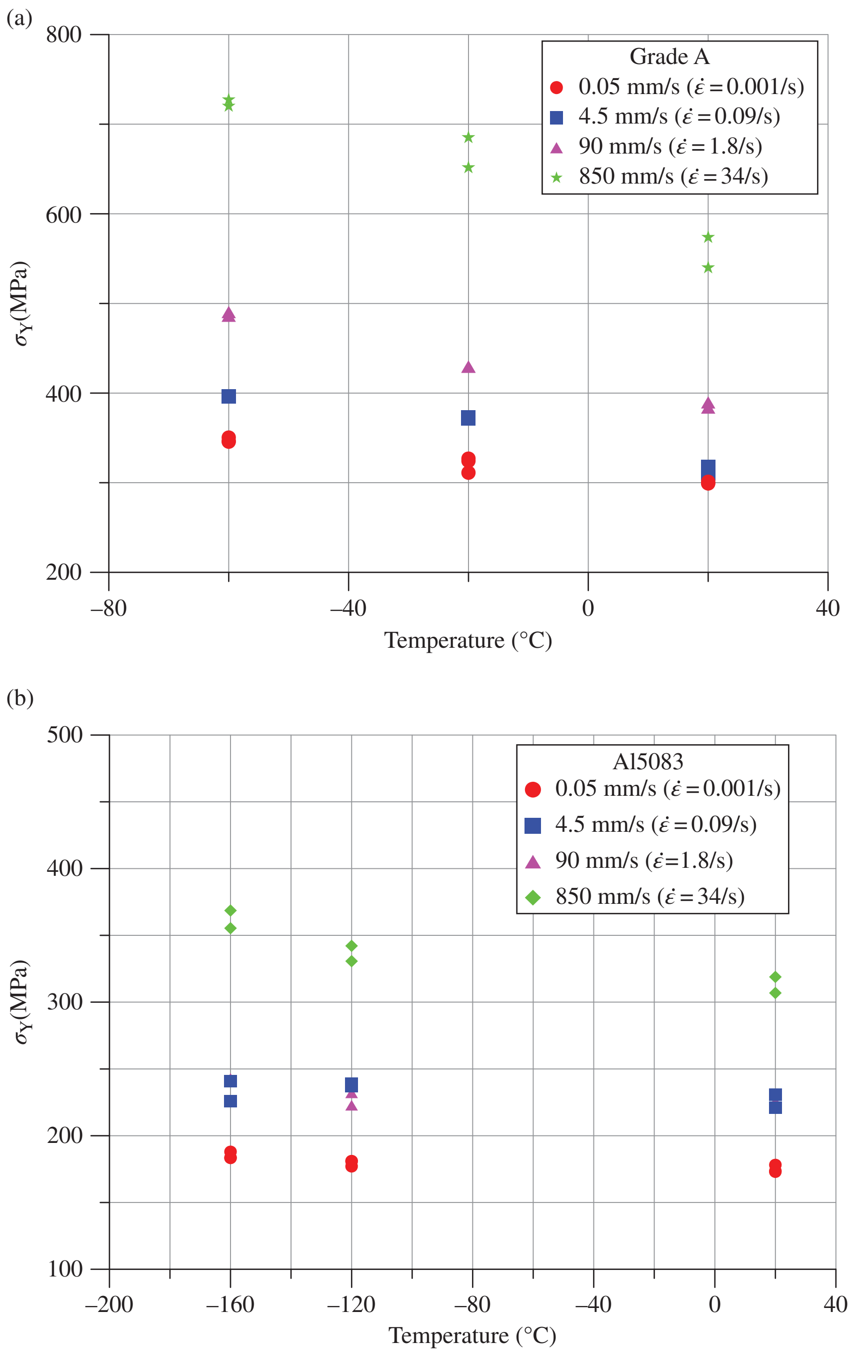

Figure 1.18 Effect of cold temperatures and strain rates on yield strength of materials: (a) mild steel (Grade A); (b) aluminum alloy 5083-O (Paik et al. 2017).

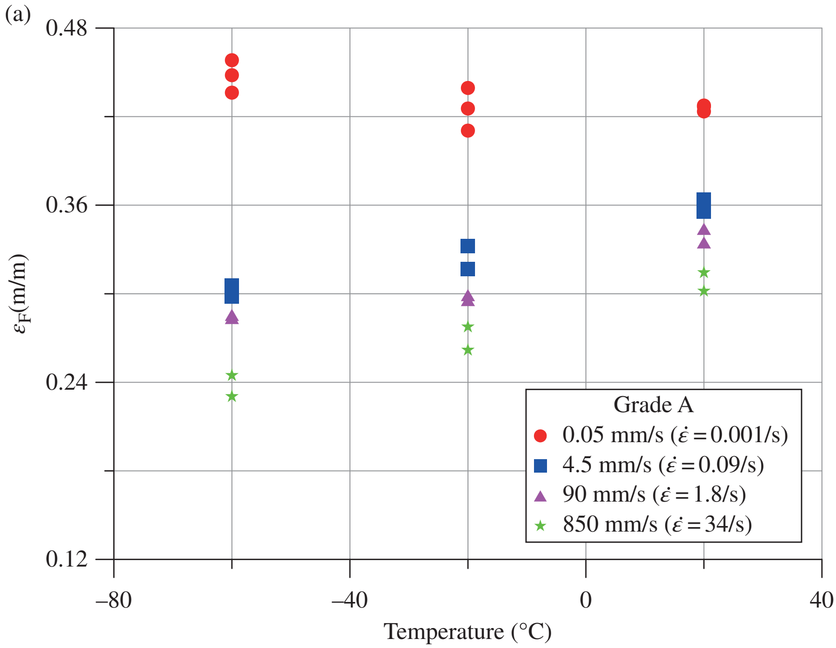

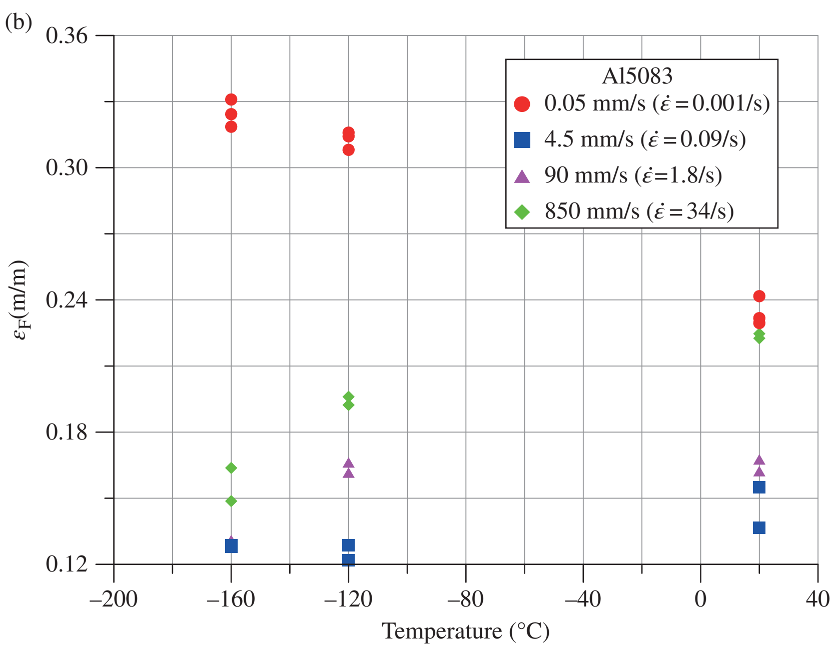

Figure 1.19 Effect of cold temperatures and strain rates on fracture strain of materials: (a) mild steel (Grade A); (b) aluminum alloy 5083-O (Paik et al. 2017).

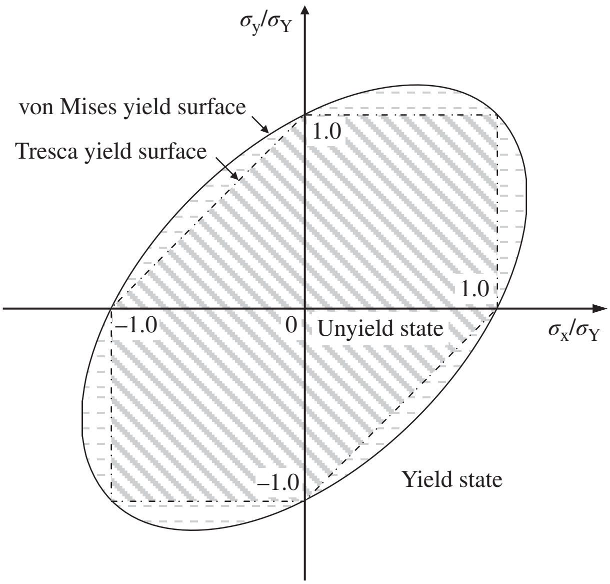

Figure 1.20 The von Mises and Tresca yield surfaces associated with two normal stress components.

3) Strain energy-based criterion (also called the Mises–Hencky or Huber–Hencky–Mises or von Mises criterion): The material yields if the strain energy due to geometric changes reaches a critical value, which corresponds to that at which the equivalent stress, σ_{eq}, reaches the yield strength, σ_Y, as determined from the uniaxial tension test as follows:

$$\sigma_{eq} = \sqrt{\sigma_x^2 - \sigma_x\sigma_y + \sigma_y^2 + 3\tau_{xy}^2} = \sigma_Y \tag{1.31c}$$

where σ_Y is the yield strength of material.

It is recognized that the first yield condition, Equation (1.31a), is relevant for a brittle material and that the last two conditions, Equations (1.31b) and (1.31c), are more appropriate for a ductile material, although the von Mises condition, Equation (1.31c), is more popular for the analysis of plated structures. Figure 1.20 illustrates the von Mises and Tresca yield surfaces associated with two normal stress components, σ_x and σ_y. The shear yield stress, τ_Y, under pure shear can be determined by solving the von Mises condition, Equation (1.31c), with regard to τ_{xy} when $\sigma_x = \sigma_y = 0$, with the result as follows:

$$\tau_Y = \frac{\sigma_Y}{\sqrt{3}} \tag{1.31d}$$

1.3.9 The Bauschinger Effect: Cyclic Loading

During operation, structural members are likely to be subjected to load cyclic effects, as shown in Figure 1.21. If a material that has been plastically strained in tension is unloaded and then strained in compression, the stress–strain curve for the compression loading

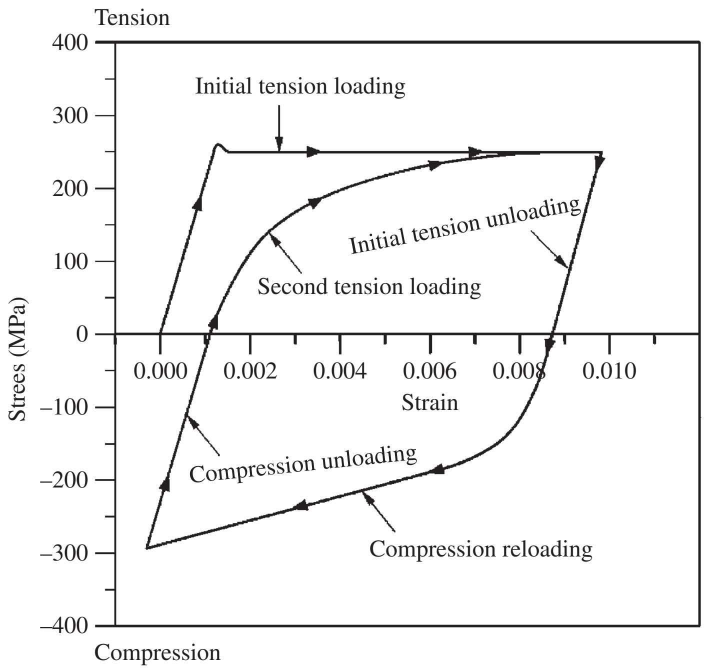

Figure 1.21 The Bauschinger effect in metals.

deviates from a linear relationship at stresses well below the yielding point of the virgin material, but it returns to the point of maximum stress and strain for the first tension loading cycle. The same effect is observed for the opposite loading cycle, that is, compression before tension. In this case, the modulus of elasticity is reduced, as shown by the shape of the stress–strain curve in Figure 1.21. This phenomenon is typically termed the Bauschinger effect (Brockenbrough & Johnston 1981). When stiffness is of primary concern, for example, in the evaluation of buckling or deflection, the Bauschinger effect may be of interest.

Within an acceptable level of accuracy, however, the mechanical properties of a particular type of steel or aluminum alloy as determined by uniaxial tension testing are also approximately accepted as being valid for the same type of the material under uniaxial compression.

1.3.10 Limits of Cold Forming

Cold forming is an efficient technique to form structural shapes, for example, a curved plate. However, it is important to realize that excessive strain during cold forming can exhaust ductility and cause cracking. Hence the strain in cold forming the structural shapes must be limited, not only to prevent cracking but also to prevent buckling collapse of structural elements subject to compressive loads. The cold-forming-induced strain is usually controlled by requiring the ratio of the bending radius to the plate thickness to be large, in the range of 5–10.

1.3.11 Lamellar Tearing

In most cases of plated structures, the behavior in the length and breadth of the plates related to load effects is of primary concern. The behavior in the wall thickness direction is normally not of interest. In heavy, welded structures, particularly in joints or connections with thick plates and heavy structural shapes, however, crack-type separation or delamination can take place in the wall thickness direction beneath the surface of plates or at weld toes. This failure is typically caused by large through-thickness strain, which is sometimes associated with weld metal shrinkage in highly restrained joints. This phenomenon is termed lamellar tearing. Careful selection of weld details, filler metal, and welding procedure and the use of steels with controlled through-thickness properties (e.g., the so-called Z grade steels) can be effective to control this failure mode.

1.4 Strength Member Types for Plated Structures

The geometric configuration of a steel- or aluminum-plated structure is determined primarily on the basis of the function of the particular structure. Figure 1.22 shows a basic part of a typical plated structure. A major difference between plated and framed structures is that the principal strength members of the former type of structure are plate panels together with support members, whereas those of the latter typically consist of truss or beam members for which the dimension in the axial direction is usually much greater than those in the other two directions.

Typical examples of plated structures are ships, ship-shaped offshore platforms, box girder bridges, and box girder cranes. Basic types of structural members that usually make up plated structures are as follows:

- Plate panels: Plating, stiffened panel, corrugated panel
- Small support members: Stiffener, beam, column, beam–column
- Strong main support members: Plate girder, frame, floor, bulkhead, box girder

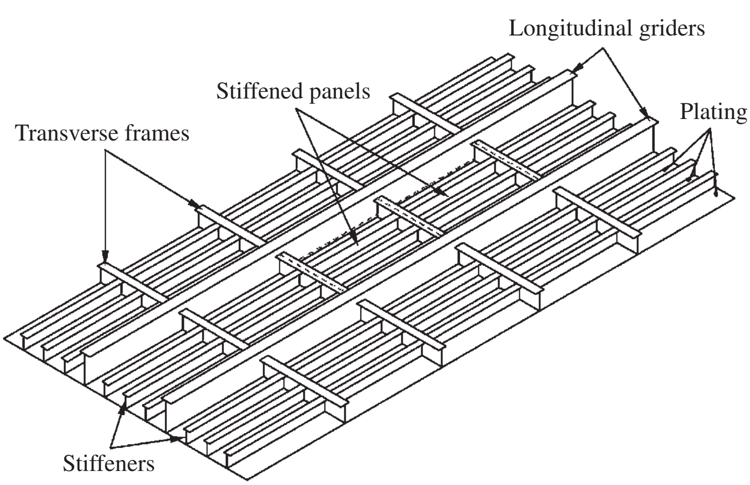

Figure 1.22 Typical plated structure.

To improve the stiffness and strength of plate panels, increasing the stiffener dimensions is usually more efficient than simply increasing the plate thickness, and thus the plate panel is usually reinforced by beam members (stiffeners) in the longitudinal or transverse direction. Figure 1.23a shows typical beam members used to stiffen the plating. A self-stiffened plate, such as the corrugated panel shown in Figure 1.23b, may also be used in some cases.

When the stiffened panels are likely to be subjected to lateral loads or out-of-plane bending or just require lateral support, they are supported by stronger beam members. Figure 1.23c shows typical strong main support members used to build plated structures. For ships and offshore structures, plate girders composed of deep webs and wide flanges are typically used for main support members. The deep web of a plate girder is often stiffened vertically and/or horizontally. Box-type support members that consist of plate panels are used for construction of land-based steel bridges or cranes. Diaphragms or transverse floors or transverse bulkheads are arranged at relevant spaces in the box girder.

Although plating primarily sustains in-plane loads, support members resist out-of-plane (lateral) loads and bending. A plate panel between stiffeners is called "plating," and plating with stiffeners is termed a "stiffened panel." A cross-stiffened panel is termed a "grillage," which in concept is essentially a set of intersecting beam members. When a one-dimensional strength member is predominantly subjected to axial compression, it is called a "column," whereas it is termed a "beam" when subjected to lateral loads or

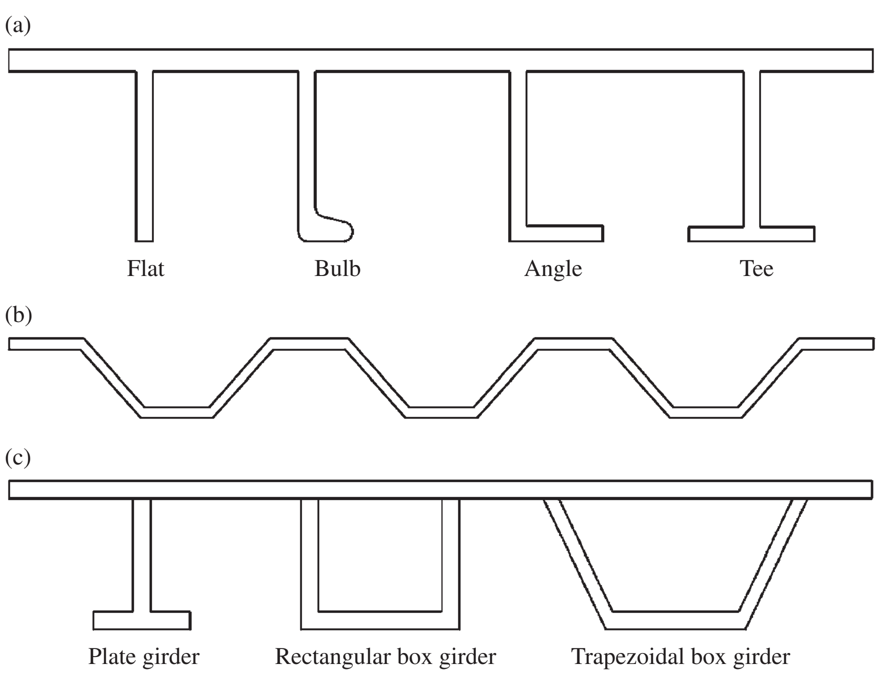

Figure 1.23 (a) Various types of beam members (stiffeners); (b) a self-stiffened plate-corrugated panel; (c) various types of strong main support members.

bending. A one-dimensional strength member under combined axial compression and bending is called a "beam–column." When the strength member is subjected to combined bending and axial tension, it is called a "tension-beam."

Strong main support members are normally called "(longitudinal) girders" when they are located in the primary loading direction (i.e., the longitudinal direction in a box girder or a ship hull girder), whereas they are sometimes called "(transverse) frames" or main support members when they are located in a direction orthogonal to the primary load direction (i.e., in the transverse direction in a box girder or a ship hull girder).

For strength analysis of plated structures, stiffeners or some support members together with their associated plating are often modeled as beams, columns, or beam–columns, as described in Chapter 2.

1.5 Types of Loads

The terminology related to the classification of applied loads for ships and offshore structures is similar to that used for land-based structures. The types of loads to which plated structures or strength members are likely to be subjected may be categorized into the following four groups:

- Dead loads
- Operational or service (live) loads
- Environmental loads
- Accidental loads

Dead loads (also called permanent loads) are time-independent, gravity-dominated service loads. Examples of dead loads are the weight of structures or permanent items that remain in place throughout the life of the structure. Dead loads are typically static and can usually be determined accurately even if the weight of some of the items may in some cases be unknown until the structural design has been completed.

Operational or service loads are typically live loads by nature with gravity and/or thermal loads that vary in magnitude and location during the normal operation of the structure. Operational loads can be quasistatic, dynamic, or even impulsive in loading speed. Examples of operational loads are the weight of people, furniture, movable equipment, wheel loads from vehicles or cargoes, and stored consumable goods. In marine structures, pressure loads due to water and cargoes and thermal loads due to cargoes (e.g., liquefied petroleum gas, liquefied natural gas) are also examples of operational loads. In the design of land-based box girder bridges, highway vehicle loading is usually separately classified under highway live loads. Although some live loads (e.g., persons and furniture) are practically permanent and static, others (e.g., box girder cranes and various types of machinery) are highly time dependent and dynamic. Because the magnitude, location, and density of live load items are generally unknown in a particular case, the determination of operational loads for design purposes is not straightforward. For this reason, regulatory bodies sometimes prescribe design service loads based on experience and proven practice.

Environmental loads are actions related to wind, current, waves, snow, and earthquake. Most environmental loads are time dependent and repeated in some fashion, that is, cyclic. Environmental loads can thus be quasistatic, dynamic, or even impulsive in loading speed. The determination of design environmental loads is often specified by regulatory bodies or classification society rules, typically using the concept of a mean return period. The design loads of snow or wind, for instance, may be specified based on a return period of 100 years or longer, indicating that extreme snowfall or wind velocity that is expected to occur once in 100 years is used in the design.

Accidental loads are actions that arise from accidents such as collision, grounding, fire, explosion, or dropped objects. Accidental loads typically have a dynamic or impact effect on structural behavior with large strains. Guidelines to predict and account for accidental loads are more meager because of the unknown nature of accidents. However, it is important to treat such loads in design, particularly when novel types of structures are involved, about which experience may be lacking. This often happens in the offshore field, where several new types of structures have been introduced in recent decades. Experimental databases in a full-scale prototype or at least large-scale models are highly required to characterize and quantify the nonlinear mechanics of structures exposed to accidental conditions, as scaling laws to convert small-scale model test results to the actual full-scale structure are not always available.

The maxima of the various types of loads mentioned previously are not always applied simultaneously, but more than one type of load normally may coexist and interact. Therefore, the structural design must account for the effects of phasing for definition of the combined loads. Usually, this involves the consideration of multiple load combinations for design, each representing a load at its extreme value together with the accompanying values of other loads. The guidelines for relevant combinations of loads to be considered in design are usually specified by regulatory bodies or classification societies for particular types of structures.

1.6 Basic Types of Structural Failure

This book is concerned with the fundamentals and practical procedures for the ULS analysis and design of steel- and aluminum-plated structures. One primary task in ULS design is to determine the level of imposed loads that cause the structural failure of individual members and the overall structure. Therefore, it is crucial to better understand what types of structural failure can primarily occur. The failure of plated structures made of ductile materials is normally related to one or both of the following nonlinear types of behavior:

- Geometric nonlinearity associated with buckling or large deflection
- Material nonlinearity due to yielding or plastic deformation

For structural members, many basic types of failure are considered, the more important of which include:

- Buckling or instability
- Plasticity in local regions
- Fatigue cracking related to cyclic loading

- Ductile or brittle fracture, given fatigue cracking or preexisting defects
- Excessive deformations

The basic failure types mentioned previously do not always occur simultaneously, but more than one phenomenon may in principle be involved until the structure reaches the ULS. For convenience, the basic types of structural failure noted previously are sometimes described and treated separately.

As the external loads increase, the most highly stressed region inside a structural member will yield first, resulting in local plastic deformation, which decreases the member stiffness. With a further increase in the load, local plastic deformation will increase and/or occur at several different regions. The stiffness of the member with large local plastic regions becomes quite low, and the displacements increase rapidly, eventually becoming so large that the member is considered to have failed.

Buckling or instability can occur in any structural member that is predominantly subjected to load sets that result in compressive effects in the structure. In buckling-related design, two types of buckling are considered, bifurcation and non-bifurcation. The former type is seen for an ideal perfect member without initial imperfections, and the latter typically occurs in an actual member with some initial imperfections. For instance, a straight elastic column has an alternative equilibrium position at a critical axial compressive load that causes a bent shape to suddenly occur at a certain value of the applied load. This threshold load, which separates into two different equilibrium conditions, is called a bifurcation load.

An initially deflected column or beam–column induces bending from the beginning of the loading contrary to the straight column, and the lateral deflection increases progressively. The member stiffness is reduced by considerable deflection and local yielding, and it eventually becomes zero at a peak load. The deflection of the member with very low or zero stiffness becomes so great that the member is considered to have collapsed. In this case, an obvious sudden buckling point does not appear until the member collapses; this type of failure is called non-bifurcation instability or limit-load buckling (Galambos 1988).

Due to repeated fluctuation of loading, fatigue cracking can initiate and propagate in the structure's stress concentration areas. Fracture is a type of structural failure caused by the rapid extension of cracks. Three types of fracture are relevant, brittle fracture, rupture, and ductile fracture. Brittle fracture normally takes place at a very small strain in materials with a low toughness or below a certain temperature, when the material's ultimate tensile strength diminishes sharply. For materials with a very high toughness, rupture occurs at a very large strain by necking of the member, typically at room temperature or higher. Ductile fracture is an intermediate fracture mode between brittle fracture and rupture. In steels or aluminum alloys, the tendency to fracture is related not only to the temperature but also to the rate at which loading is applied. The higher the loading rate, the greater the tendency toward brittle fracture.

1.7 Fabrication Related Initial Imperfections

Welded metal structures always have initial imperfections in the form of initial distortions, residual stresses, or softening in the weld fusion zone or HAZ. Because such fabrication related initial imperfections may affect the structural properties and